UNIVERSITÀ
DEGLI STUDI
DI PADOVA

DIPARTIMENTO
DI INGEGNERIA
DELL'INFORMAZIONE

DIPARTIMENTO DI INGEGNERIA DELL'INFORMAZIONE

CORSO DI LAUREA MAGISTRALE IN

Ingegneria Elettronica

"Textile Antennas for Wearable Application in the 863-870 MHz Frequency Range: Design, Fabrication and Performance Analysis"

Relatore: Prof. Marco Santagiustina

Laureanda: Laura Bortolami

ANNO ACCADEMICO 2023 – 2024

Data di laurea: 10 Luglio 2024

TABLE OF CONTENTS

ABSTRACT

Wearable systems offer an effective solution to seamlessly integrate functionalities such as sensing, communication, and localization by implementing the components directly on the fabric or on the wearable device itself. This innovative technology is widely used across numerous IoT applications and fields revolutionizing our everyday lives by improving comfort and portability while simplifying implementation and usage. In health care, wearables systems are extensively employed for monitoring patients' vital data and transmitting it through wireless communication technologies. They are also widely used in sports for monitoring athlete performances enabling GPS tracking and navigation assistance. Additionally, in military applications, wearables technology provides secure and reliable communication in the field.

These systems seamlessly integrate both the sensing components and the communication system creating a compact, lightweight, and portable solution enhancing the overall usability and practicality of the device. The key element of the wearables systems lies in textile antennas.

This work aims to present the design and implementation process of two different types of embroidered textile antennas tailored to be integrated into a smart textile system.

The proposed antennas include a bow tie textile antenna based on Sierpinsky geometry and a dipole textile antenna both designed to work at 868 MHz.

A simulation analysis is conducted using CST to tune the central frequency of both antennas and determine the appropriate dimensions necessary to start the fabrication process. Even though the results of a numerical tool (CST) provide valuable insights, certain limitations are identified and will be further addressed.

During the fabrication process, several challenges emerged, in particular ensuring consistent and reliable conductivity of the conductive thread across the embroidered pattern. Variations in thread properties and stitching techniques strongly impact the resonant frequency and so the antenna's performance.

Based on the analysis, two textile antenna models were crafted for easy hand-embroidering onto a substrate for wearable applications and implemented in a body temperature monitoring system with LoRa connectivity. Additionally, a workshop was conducted in Regensburg, Germany where young students successfully embroidered their antennas, showing the accessibility and ease of implementing smart textiles and textile electronics for diverse solutions.

List of Tables

List of Figures

1

Antenna Theory

1.1 Background

Antennas are fundamental components of wireless communications, playing a crucial role in transmitting and receiving electromagnetic waves. They are used in various applications, including radio broadcasting, television, mobile communications, satellite communications, radar, and more.

An antenna converts electrical power into electromagnetic waves and vice versa. It provides a transition from a guided wave on a transmission line to free space wave (or viceversa).

Antennas operate over a wide range of frequencies, from a few kHz for radio frequencies to hundreds of GHz for satellite communications.

When it comes to choosing proper antennas for specific wireless communication systems, factors related to power loss and transmission efficiency must be taken into account. For a transmitter-receiver distance R, the power loss in a transmission line is proportional to $(e^{-\alpha R})^2$, where α represents the attenuation constant of the transmission line. On the other hand, when an antenna is used in a line-of-sight configuration, the power loss is proportional to $\frac{1}{R^2}$. These considerations are essential for ensuring effective communication over varying distances and frequencies.

Generally speaking at low frequencies transmission lines are practical but, when distances are large and frequencies are increased, the signal losses are no longer tolerable, the costs of a transmission line becomes large and the use of an antenna is preferable. It needs to be mentioned that an important exception is the fiber optic transmission line where losses are very low.

In many application fields, a wirless communication system is strictly necessary and antennas must be used. For example, mobile communication involving aircraft, ships or land vehicles that require to transmit or receive information. There are also non-communication applications for antennas such as remote sensing which can be active (e.g. radar) or passive (e.g. radiometry). The received signals contain information about objects, scenes, or localization, all very important in industrial applications.

The theoretical foundations for antennas rest in Maxwell equations that describe the behavior of electric and magnetic fields in space.

Most antenna application have a sinusoidally varying source (ρ, J), therefore for the time varying fields at a radiant frequency ω, the phasor form of Maxwell's equations are :

$$\nabla \times \boldsymbol{E} = -j\omega \boldsymbol{B} \quad [1\text{-}1]$$

$$\nabla \times \boldsymbol{H} = j\omega \boldsymbol{D} + \boldsymbol{J_T} \quad [1\text{-}2]$$

$$\nabla \cdot \boldsymbol{D} = \rho \quad [1\text{-}3]$$

$$\nabla \cdot \boldsymbol{B} = 0 \quad [1\text{-}4]$$

$$\nabla \cdot \boldsymbol{J_T} = -j\omega\rho \quad [1\text{-}5]$$

In addition, to consider the characteristics of the medium, the following two relations needs to be addressed:

$$\mathbf{D} = \varepsilon \mathbf{E} \quad [1\text{-}6]$$

$$\mathbf{B} = \mu \mathbf{H} \quad [1\text{-}7]$$

The permittivity ε and permeability μ of a material are expressed as the product of their relative values and the respective properties of free space as follows:

$$\varepsilon = \varepsilon_r \, \varepsilon_0 \quad [1\text{-}8]$$

$$\mu = \mu_r \, \mu_0 \quad [1\text{-}9]$$

Where ε_0 and μ_0 are the permittivity and permeability in free space respectively.

$$\varepsilon_0 = 8.854\ 10^{-12} \left[\frac{F}{m}\right] \quad [1\text{-}10]$$

$$\mu_0 = 4\pi\ 10^{-7}\ \left[\frac{H}{m}\right] \qquad [1\text{-}11]$$

The quantities $\boldsymbol{E}$, $\boldsymbol{H}$, $\boldsymbol{D}$ and $\boldsymbol{B}$ describe the physical terms of electric and magnetic field amplitudes and the electric and magnetic induction field densities, respectively. The vector $\boldsymbol{J_T}$ is the total current density which is composed by an impressed $\boldsymbol{J}$ (or source) and a conduction $\rho\boldsymbol{E}$ current density.

$$\boldsymbol{J_T} = \boldsymbol{J} + \rho\boldsymbol{E} \qquad [1\text{-}12]$$

If more than one frequency is present, the time-varying field needs to be extracted from [1-1,2] as a function of frequency, but since in antenna problems, the bandwidth of the signals is very small, this is not necessary. Usually, a carrier frequency comes with some sort of modulation giving a spread of frequency around the carrier.

In order to simplify the process of finding the solution for $\boldsymbol{E}$ and $\boldsymbol{H}$ with a given **J** (which is a known term in the equations since it's the signal to be transmitted), they can be expressed in relation with a single quantity, the magnetic vector potential $\boldsymbol{A}$ according to:

$$\boldsymbol{H} = \frac{1}{\mu_0}\ \nabla \times \boldsymbol{A} \qquad [1\text{-}13]$$

$$\boldsymbol{E} = -j\omega\boldsymbol{A} + \frac{\nabla(\nabla\cdot\boldsymbol{A})}{j\omega\mu_0\varepsilon_0} \qquad [1\text{-}14]$$

Rearranging Maxwell equations with respect to the $\boldsymbol{A}$ and the electric scalar potential ϕ the following (Helmoholts and Poisson) equations are obtained:

$$\nabla^2\boldsymbol{A} + \omega^2\mu_0\varepsilon_0\ \boldsymbol{A} = -\mu_0\boldsymbol{J} \qquad [1\text{-}15]$$

$$\nabla^2\phi\ \omega^2\mu_0\varepsilon_0\ \phi = -\frac{\rho}{\varepsilon_0} \qquad [1\text{-}16]$$

To calculate the radiation (electric and magnetic field) from an antenna is necessary to solve [1-15] and [1-16] and derive the fields with [1-13] and [1-14].

This involves applying the equations to the particular antenna under study, taking into account various factors such as the boundary conditions, the antenna's geometry, and the properties of the surrounding medium.
Due to the vast number of antennas and the complex geometries that some antennas exhibit, analytical calculations may not always be possible. In such cases, numerical methods and computational techniques become essential tools for antenna analysis and design. These methods involve breaking down the problem into discrete elements or regions and applying numerical algorithms to approximate the solution.

A multitude of antenna types exist, each tailored to specific applications and requirements. Antennas vary widely in their design, configuration, and operating principles, reflecting the diverse needs of different communication, broadcasting, radar, and sensing systems. From the simple dipole and Yagi-Uda antennas used in radio and television broadcasting to the sophisticated phased array antennas employed in radar and satellite communications. Whether it's for wireless networking, mobile phones, satellite navigation, or deep space communication there exists a set of antenna designs optimized to meet the unique demands of each application. In the following section three types of antenna will be addressed: Microstrip patch antennas, Aperture antennas and the Yagi-Uda array antenna.

MICROSTRIP PATCH ANTENNA

A microstrip patch antenna is a type of antenna that is widely used due to its low profile, lightweight, and ease of fabrication. It's particularly popular in applications where a compact and conformal design is required.
It consists of three main layers:

- Radiating patch: Flat metal patch made of conducting materials (e.g. copper). It can take various shapes, most commonly rectangular or circular.
- Dielectric substrate: Dielectric layer placed between the patch and the ground plane. The dielectric material can be Teflon or, in wearable antennas, Cotton. Its permittivity ε_r and thickness affect the antenna's performance.

- Ground Plane: it's a metal layer on the opposite side of the dielectric substrate providing a return path for the current.

The patch antenna belongs to the class of resonant antennas; it operates by resonating the patch at a specific frequency, creating a strong electric field between the patch and the ground plane. This field radiates outwards as electromagnetic waves. They are typically used at frequencies from 1 to 100 GHz. The conductive patch can be manufactured using standard printed circuit board (PCB) technology, which is cost-effective and scalable and can be mounted on curved surfaces (dielectric layer) making the antenna suitable for wearable applications.

Microstrip patch antennas typically have a narrow bandwidth, which can limit their application in broadband systems but techniques such as using thicker substrates or using multiple resonant elements can enhance it.

Compared to other types of antennas, such as parabolic reflectors or horn antennas, they generally have lower gain.

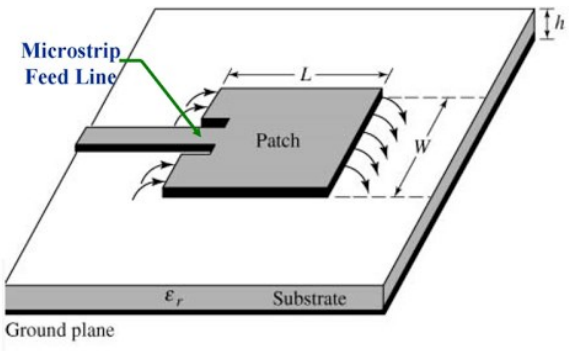

Fig 1.1: Rectangular microstrip patch antenna

APERTURE ANTENNAS

An aperture antenna is designed with an opening that facilitates the transmission or reception of electromagnetic waves. This opening can take various forms such as slots, waveguides, horns, reflectors, or lenses. Aperture antennas are well-suited for high-frequency applications, making them ideal for advanced communication systems and radar, for example for aircraft and spacecraft applications. They can be seamlessly integrated into the surface of the vehicle, with the opening covered by a dielectric material that permits the passage of electromagnetic energy.
To understand the distant radiation patterns, it's necessary to know the surface currents flowing on the antenna radiating surfaces. However, knowing these current distributions can be challenging, and often require approximations or experimental measurements. Applying the *field equivalence principle,* it's possible to make reasonable estimations of the electromagnetic fields around the physical antenna aperture.
Such principle states that the actual sources on the antenna aperture can be replaced by equivalent sources on an external closed surface that is physically outside the antenna aperture.

The main feature of a large aperture antenna is the increase in gain with the operating frequency which means they can transmit or receive signals over long distances along precise and narrow directions and high radiation efficiency. The gain of the aperture antenna can be estimated using the universal formula linking gain G to effective area A_e:

$$G = \frac{4\pi}{\lambda^2} A_e \qquad [1\text{-}17]$$

Aperture antennas typically provide directional radiation patterns, which can be tailored to specific requirements for signal focus and coverage. Their directional radiation patterns help in reducing interference with other, nearby antennas or electronic devices, enhancing overall system performance.

a)

b)

Fig 1.2: a) Horn antenna b) Parabolic reflector

YAGI-UDA ARRAY ANTENNA

The Yagi-Uda array antenna, commonly referred to as the Yagi antenna, is a highly directional antenna that is widely used in applications requiring high gain and focused radiation patterns. It was invented by Japanese engineers Hidetsugu Yagi and Shintaro Uda in the 1920s.
It consists of a parasitic linear array of parallel dipoles. The parasitic elements are not directly driven but they receive their excitation by near-field coupling from the driven elements.
These parasitic elements are called the “reflector” and the “directors”. The reflector is on the far left in Fig 1.4 and the directors are all of the elements starting from the third element from the left and continuing to the right side.

The driven element of a Yagi antenna is the component where the feed line from the transmitter is connected, allowing power to be transferred to the antenna. For a dipole driven element to be “resonant,” its electrical length must be about half the wavelength of the frequency applied to its feed point.

In a Yagi antenna, the director elements are the shortest parasitic elements and are positioned at the front, facing the receiving station. These directors are tuned to a slightly higher frequency

than the driven element, making them about 5% shorter than the driven element. The exact lengths of the directors can vary depending on factors like their spacing, the number of directors, the desired radiation pattern, the pattern's bandwidth, and the diameter of the elements. The number of directors that can be added is limited by the length of the supporting boom. Directors are crucial for providing the antenna with a directional pattern and increasing its gain.

The reflector's resonant frequency is lower, and its length is approximately 5% longer than the driven element.

The Yagi antenna has an intense main lobe that points towards the directors. This is where most of the radiated power is concentrated, providing high gain and making the antenna highly directional. The secondary side lobes on either side of the main lobe are generally minimized to reduce interference from unwanted directions.

The antenna can be oriented for horizontal or vertical polarization depending on the application. This is determined by the orientation of the elements.

Its high gain and directional properties make the antenna highly effective for television reception, particularly in VHF and UHF bands. Additionally, Yagi antennas are employed in wireless networks to extend coverage, in public safety and emergency services to ensure robust and far-reaching communication. Their use also extends to radar systems, scientific research, and even military applications, where directional capabilities are essential.

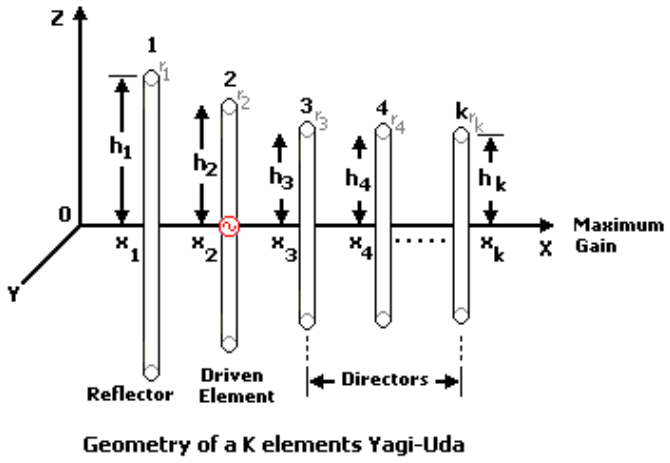

Fig 1.3: Yagi-Uda array antenna

1.2 ANTENNA FUNDAMENTAL PROPERTIES

To effectively evaluate an antenna's performance, it's important to define key parameters that govern its behavior. These parameters are often interrelated and their understanding is essential to comprehensively assess an antenna's performance and capabilities. Observing technical specifications concerning these parameters is crucial when designing an antenna.
In the following section, the main features of an antenna will be reviewed.

RADIATION PATTERN

An antenna *radiation pattern* or *antenna pattern* is defined as "a mathematical function or a graphical representation of the radiation properties of the antenna as a function of space coordinates. In most cases, the radiation pattern is determined in the far field region (i.e for $r>>2D^2/\lambda$ with D being the largest dimension of the antenna) and is represented as a function of the directional coordinates. Radiation properties include power flux density, radiation intensity, field strength, directivity, phase or polarization".[1]
A radiation pattern can represent several quantities, such as gain, directivity, electric field or radiation vector. Consequently, the terms gain pattern, electric field pattern or radiation vector pattern are used, respectively.
In other words, the radiation pattern determines the direction and strength of electromagnetic radiation for an antenna and it can be represented in either a three-dimensional (i.e. function of (θ, ϕ, r)) or two-dimensional image. In the latter case, the radiation pattern represents a cut of the 3D radiation pattern, with a plane passing through the origin of the reference frame (where the antenna is located).
There are two main representations: the *field* pattern and the *power* pattern.
The *field* pattern traces the amplitude of the received electric or magnetic field at a constant distance from the antenna. It provides insight into how the field strength varies in different directions around the antenna.

It can be constructed by drawing the following surface:

$$[|F(\theta,\phi)|,\theta,\phi] \qquad [1\text{-}18]$$

where θ and ϕ are the latitude and longitude of spherical coordinates and $F(\theta,\phi)$ is defined as the *normalized field pattern function*:

$$F(\theta,\phi) \equiv \frac{E(r,\theta,\phi)}{E(r,\theta_{MAX},\phi_{MAX})} \qquad [1\text{-}19]$$

where $E(r,\theta_{MAX},\phi_{MAX})$ is the field in the direction θ_{MAX}, ϕ_{MAX} of the maximum modulus $max\ (|E|)$.

On the other hand, the *power* pattern illustrates the spatial distribution of power density along a fixed distance from the antenna. It indicates how the power radiated by the antenna is distributed in space, providing information about the relative strength of the radiated signal in different directions.

It can be constructed by drawing the following surface:

$$[|F(\theta,\phi)|^2\theta,\phi] \qquad [1\text{-}20]$$

The power pattern can be plotted in a linear scale or logarithmic scale.

Often the field and power patterns are normalized with respect to their maximum value, yielding normalized field and power patterns.

Figure 1.4 shows three examples of a Field and Power pattern (dB and linear scale).

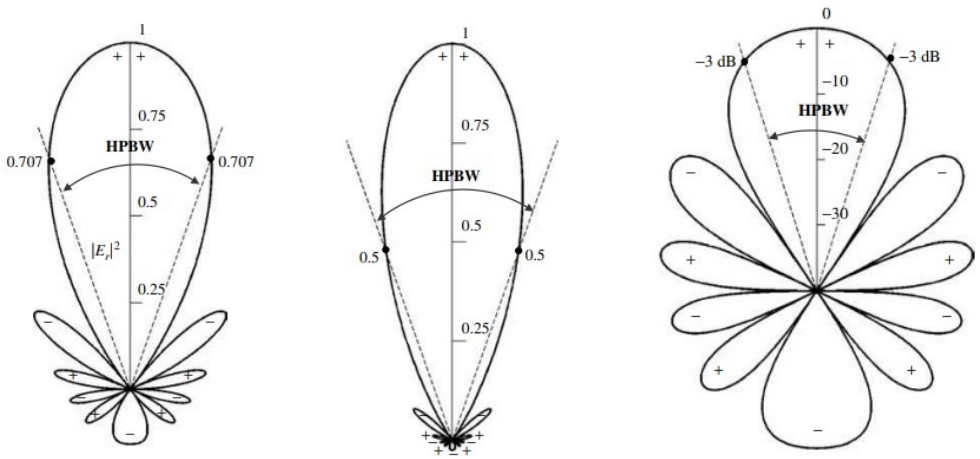

a) *b)* *c)*

Fig 1.4: Example of radiation pattern a) Field pattern (linear scale) b) Power pattern (linear scale) c) Power pattern (dB)

DIRECTIVITY

The directivity of an antenna is defined as "the ratio of the radiation intensity in a given direction from the antenna to the radiation intensity averaged over all directions. The average radiation intensity is equal to the total power radiated by the antenna divided by 4π. If the direction is not specified, the direction of maximum radiation intensity is implied."[2]

In other words the directivity D can be defined as the ratio of the radiated power per unit solid angle to its average value U_{AVG} :

$$D(\theta,\phi) = \frac{U(\theta,\phi)}{U_{AVG}} = \frac{|F(\theta,\phi)|^2}{\frac{1}{4\pi}\iint |F(\theta,\phi)|^2 \, d\Omega} \qquad [1\text{-}21]$$

Equation [1-21] shows that directivity is entirely determined by the pattern shape.

When directivity is mentioned as a single number without reference to a direction (θ,ϕ), maximum directivity is usually intended.

$$D = \frac{U_m}{U_{AVG}} = \frac{EIRP}{P} \qquad [1\text{-}22]$$

where U_m is the maximum radiation intensity.

An alternative definition is given by the ratio between the effective isotropic radiated power $EIRP$ and the total radiated power P.
The *EIRP* is the power radiated by an isotropic source generating at a distance r the same $|E_{max}|$ of the antenna of directivity *D*. Directivity is always larger than 1 by definition.
The directivity refers to the antenna ability to focus electromagnetic energy in a particular direction; it quantifies how well an antenna can transmit or receive signals in a specific direction compared to an isotropic radiator, which would radiates energy equally in all directions.

GAIN AND RADIATION EFFICIENCY

The Gain (or power gain) of an antenna (in a given direction) is defined as "the ratio of the intensity, in a given direction, to the radiation intensity that would be obtained if the power accepted by the antenna were radiated isotropically. The radiation intensity corresponding to the isotropically radiated power is equal to the power accepted (input) by the antenna divided by 4π."[2].
In equations:

$$G = \frac{U_m}{P_{in}/4\pi} = \frac{EIRP}{P_{in}} \qquad [1\text{-}23]$$

The gain is related to the directivity through the *Radiation efficiency* which is defined as the ratio between the radiated power and the power supplied at the input port of the antenna.

$$e_r = \frac{P}{P_{in}} \qquad [1\text{-}24]$$

Therefore:

$$G = e_r\, D \qquad [1\text{-}25]$$

Equation [1-23] accounts that not all the power supplied to the antenna will be radiated, part of the input power will be dissipated. The radiation efficiency quantifies how well the input power is radiated and its value is always between 0 and 1.

INPUT IMPEDANCE

The *Input impedance* is defined as "the impedance presented by an antenna at its terminals or the ratio of the voltage to current at a pair of terminals or the ratio of the appropriate components of the electric to magnetic fields at a point." [2]. The primary focus lies in the input impedance at the pair of terminals which are the input terminals of the antenna.
Input impedance is composed by real and imaginary parts:

$$Z_A = R_A + jX_A \qquad [1\text{-}26]$$

Where the input resistance R_A represents the active (mean) power and the input reactance X_A represents the power stored in the near field of the antenna.
The input resistance represents both radiated power i.e. energy that leaves the antenna and does not return, and Ohmic losses, which are associated to heating in the antenna structures. On many antennas Ohmic losses are much lower than radiation losses, however, Ohmic losses are usually significant on electrically small antenna which have dimensions much less than a wavelength.
The input impedance of an antenna is generally a function of frequency meaning that the antenna will be matched to the interconnecting transmission line and other associated equipment only within a certain bandwidth.
It's influenced by various factors such as the antenna shape, how it's driven, and its surroundings; due to the complexity and variety of their shapes, only a few antennas have been thoroughly analyzed analytically (e.g. dipole antenna). For most antennas, the input impedance is determined through experimental methods (e.g. Quasi-static method, Tapered transmission line method) or measurements [3].

BANDWIDTH

The *bandwidth* of an antenna is defined as "the range of frequencies within which the performance of the antenna, with respect to some characteristic, conforms to a specified standard."[2]
In other terms, the bandwidth of an antenna refers to the range of frequencies surrounding a center frequency, typically the resonance frequency for a dipole antenna. Within this range, the

antenna's characteristics, such as input impedance, radiation pattern, beamwidth, and efficiency, remain within acceptable values compared to those at the center frequency.

The bandwidth as a percent of the central frequency is defined as :

$$B_p = \frac{f_u - f_L}{f_c} \times 100\% \qquad [1\text{-}27]$$

Another definition for bandwidth is :

$$B_r = \frac{f_u}{f_L} \qquad [1\text{-}28]$$

Where f_u and f_L are the upper and lower frequencies of operation for which satisfactory performance is obtained.

In many applications, an antenna must operate effectively over a wide range of frequencies and a broad band antenna is needed. In other words, the term *broadband* lacks a precise definition and can vary depending on the specific antenna in question. However, it generally applies to an antenna when its impedance and radiation pattern remain relatively stable over a frequency range of approximately an octave (B_r=2) or more.

RETURN LOSS

Return loss in an antenna refers to the ratio of power reflected from the antenna compared to the power that is incident upon it. It is usually expressed in decibels (dB) and it's a measure of the efficiency with which the antenna can transfer power to the transmission line or medium. It characterizes how well the antenna is matched to the transmission line or feed system. A higher return loss indicates better matching between the antenna and the transmission line, resulting in less power being reflected back towards the source.

The Return loss expressd in decibel is defined as :

$$RL(dB) = -10 \times log_{10}\left(\frac{P_{reflected}}{P_{incident}}\right) \qquad [1\text{-}29]$$
$$= -20\, log_{10}(\Gamma)$$

Where Γ is the reflection coefficient, $P_{reflected}$ and $P_{incident}$ are the power reflected from the antenna and the power incident upon it respectively.

For a perfect match ($P_{reflected} = 0$), RL would be infinite, indicating no power is reflected back, which is the ideal scenario for an antenna system.

An equivalent way to indicate how well an antenna is matched to the transmission line or feed system is by evaluating the S11 parameter.

$$S11 = 20\ log_{10}(\Gamma) = -RL \qquad [1\text{-}30]$$

The negative sign of RL is frequently omitted in graphical representations of the return loss formula, leading to interchangeability with the S_{11} parameter.

For example when S11 is at -10dB, it means that at least 90% of the input power is effectively delivered to the device, with less than 10% being reflected back.

Voltage Standing Wave Ratio (VSWR) is essentially an alternative representation of Return Loss. VSWR is a reference to the actual voltages that are created within a transmission line system when there are forward and reflected radio waves propagating simultaneously:

$$VSWR = \frac{1+|\Gamma|}{1-|\Gamma|} \qquad [1\text{-}31]$$

A lower VSWR value indicates better impedance matching, with less power being reflected back towards the source. Conversely, a higher VSWR value indicates poorer matching and greater power loss due to reflections.

POLARIZATION

Polarization describes the vector nature of the electric fields radiated by an antenna. The figure traced out with time by the tip of the instantaneous electric field vector determines the polarization of a wave.

The polarization of waves radiated by an antenna will vary with direction. Usually, the polarization characteristics of an antenna remain relatively constant over its main beam and the

polarization on the main beam is used to describe the antenna polarization. Reciprocal antennas have identical radiation patterns on transmitting and receiving.

Specific antenna applications may have polarization requirements based on factors such as interference environment, and compatibility with other equipment.

For example, satellite communication systems may require circular polarization to ensure reliable communication with satellites in orbit.

If the electric field vector moves back and forth along a line, it is said to be *linearly polarized*. It can be *horizontal* if the electric field vector is aligned parallel to the ground plane, or *vertical* if it is aligned perpendicular to the ground plane.

An example is the electric field from an ideal dipole antenna or any linear current.

If the electric field vector remains constant in amplitude but rotates around a circular path it is *circularly polarized*. *Left-hand* (LHCP) circularly polarized if it rotates clockwise and *right-hand* (RHCP) circularly polarized if it rotates counterclockwise, on a plane viewed from the direction of propagation.

Finally, if the electric field vector of the electromagnetic wave follows an elliptical path as it propagates, it is *elliptically polarized*. Like for the circular polarization, the elliptical can be further categorized in Left-hand (LHEP) and Right-hand (RHEP).

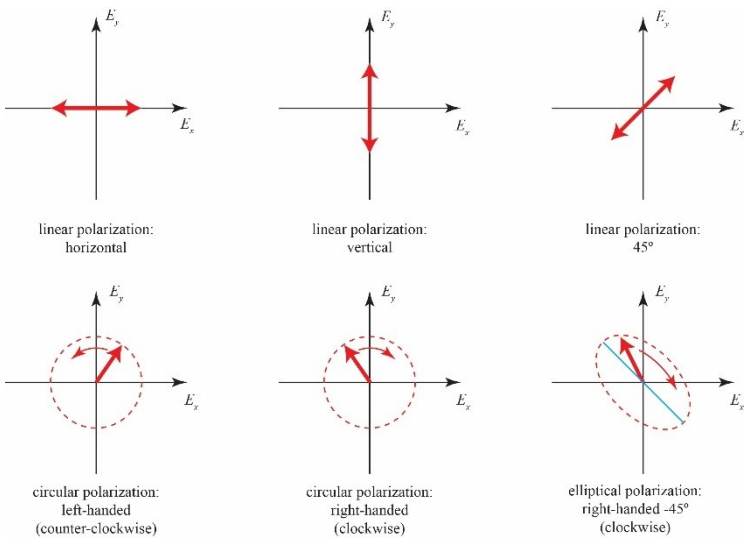

Fig 1.5: Polarization states

1.3 DIPOLE ANTENNA

Among the various antenna designs available, the dipole antenna stands out due to its simplicity, effectiveness, and versatility. A dipole antenna is one of the most fundamental types of antennas and serves as a foundational model for understanding more complex antenna structures.

A dipole antenna consists of two conductive elements, typically metal rods or wires, which are arranged in a straight line and are fed with an alternating current at the center gap. It's symmetric, meaning each half of the antenna is identical in length and shape. This symmetry helps to create a balanced radiation pattern with very clean linear polarization, which is one of the reasons for its widespread use.

For the purpose of this thesis, particular attention will be given to the half-wave dipole antenna.

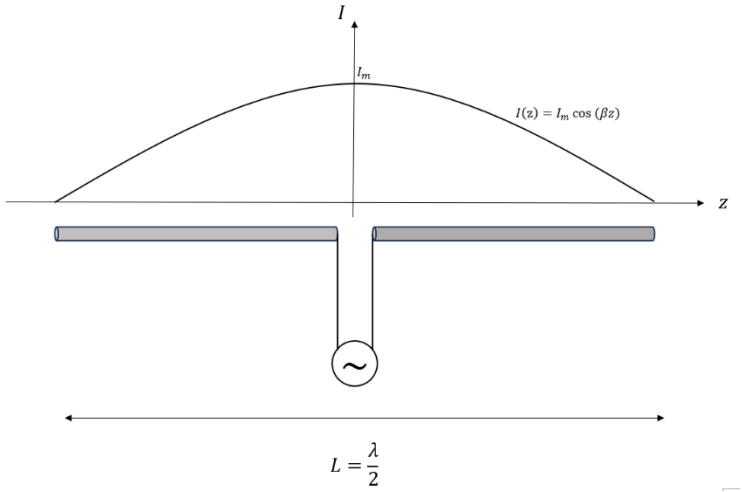

Fig 1.6: Half-wave dipole antenna

To derive the expression for the current distribution on a half-wave dipole antenna [1-32] from the general expression for a generic wire dipole antenna [1-33], the length of the dipole must be imposed equal to half the wavelength.

$$I(z) = -I_m \frac{\sin\beta\left(|z|-{}^{L}/_{2}\right)}{\sin\beta\,{}^{L}/_{2}} \qquad L = \frac{\lambda}{2} \qquad [1\text{-}32]$$

$$I(z) = I_m \cos(\beta\, z) \qquad [1\text{-}33]$$

The current distribution is that of a standing wave approximately sinusoidal along the length of the dipole with its maximum value I_m at the center of the dipole as shown in Figure 1.6.
Once the current distribution expression [1-33] is known, the complete electric and magnetic far fields can be calculated as follows:

$$E_\theta = j\frac{\eta_0 I_m \cos\left[\frac{\pi}{2}\cos\theta\right]}{2\pi \sin\theta}\ \frac{\exp(-j\beta r)}{r} \qquad [1\text{-}34]$$

$$H_\theta = \frac{E_\theta}{\eta_0} \qquad [1\text{-}35]$$

From [1-34] and [1-35] several parameters can be calculated such as the field pattern function by [1-19], directivity by [1-21] and radiation resistance:

$$F(\theta) = \frac{\cos[\pi/2\ cos\theta]}{sin\theta} \qquad [1\text{-}36]$$

$$D = \frac{4\pi U_m}{P} = 1.64 = 2.15\ dB \qquad [1\text{-}37]$$

$$R = \frac{2.44\,\eta_0}{4\pi} \cong 73\ \Omega \qquad [1\text{-}38]$$

The directivity of a half wave dipole antenna is only slightly greater of the directivity value of 1.5 for an ideal dipole with a uniform current.
From [1-36] it's possible to derive the radiation pattern. It is omnidirectional on the plane orthogonal to the dipole (H-plane) and with two lobes on the E-planes.
It is represented in Fig. 1.7a, by the direction $\theta = 90°$.

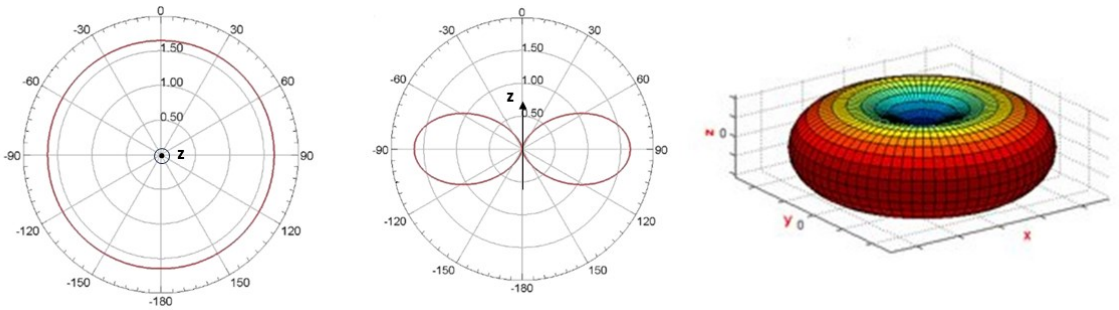

a) *b)* *c)*

Fig 1.7: Radiation pattern of a half dipole antenna a) H_plane b) E-plane c) 3D linear scale gain

The radiation resistance of [1-38] is also the resistance at the input terminals (input resistance) since the Ohmic losses are usually negligible.

The input impedance for half wave dipole is derived as :

$$Z_A = 73 + j45.5\ \Omega \qquad [1\text{-}39]$$

As shown in Fig (1.8) the input reactance is zero for antenna length L slightly shorter than λ/2. This is called a half-wave resonant dipole.

For such antenna, the input impedance is almost real and equal to the characteristic impedance of standardized coaxial cables (75 Ω), so the connection between the half-wave resonant dipole and the coaxial cable is very close to the condition of impedance matching. No matching network is actually required. The reactive power goes to zero and the mean electric and magnetic energies are equal; the antenna achieves resonance. In this condition the antenna operates at its most efficient point, with maximum power being radiated.

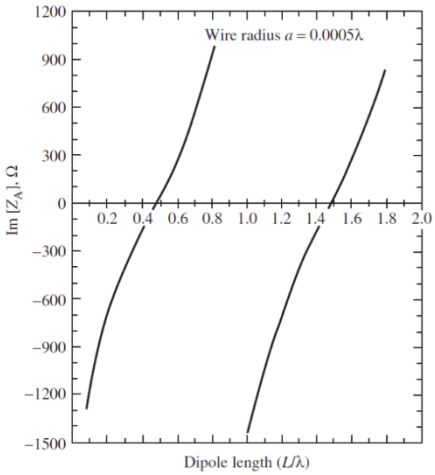

Fig 1.8: Input reactance of a center-fed wire dipole of radius 0.0005 λ as a function of length L.

Since dipoles are resonant structures, they inherently have a narrow bandwidth. However, increasing the thickness of the wire used in the dipole can effectively increase the bandwidth as show in Fig (1.9).

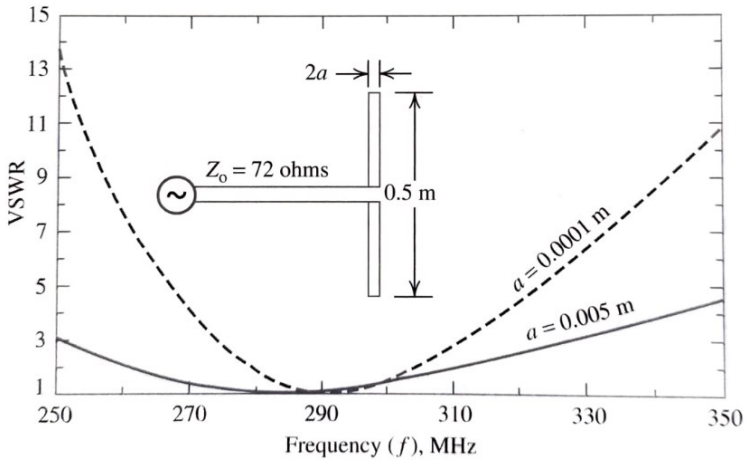

Fig 1.9: VSWR as a function of frequency for dipoles of different wire diameters

This is why patch dipole antennas are widely used.

Patch antennas, also known as microstrip antennas, are designed to overcome the bandwidth limitations of traditional wire dipole antennas. These antennas feature a flat, rectangular (or other shapes) conductive patch on a ground plane separated by a dielectric substrate. This configuration not only offers a more compact and low-profile design but also significantly increases the bandwidth compared to conventional wire dipole antennas.

1.4 BOW TIE ANTENNA

In the recent years, there has been a growing need for integrated, low-profile antenna designs in the ultra-wideband domain for various applications, as well as new technologies.

Especially for portable devices, one critical issue is the size and compactness of the antenna structure, as it directly impacts the bandwidth and gain.

An example is the “Bow tie” antenna; a thoroughly researched wideband, coplanar antenna known for its low-profile design which makes it easy to fabricate.[4]

Additionally, its simple design is compatible with planar feeding systems, making them widely used in both theoretical research and engineering applications.

When discussing broadband antennas, it’s noted that the frequency bandwidth of a simple dipole antenna can be enhanced by using thicker wire, as shown in Fig. (1.10). [4]

Applying this concept, the antenna bandwidth can be further increased by flaring the conductors to create a biconical structure and eventually a flat bow tie antenna.

The bow-tie antenna is a planar version of the finite biconical antenna with a much simpler configuration. It can be implemented using different structures, including wire antennas [5] and patch antennas [6], both having similar radiation characteristics and they can be designed for various frequency bands and applications. The choice between them often depends on factors such as size constraints, fabrication techniques, and performance requirements.

Its omnidirectional radiation pattern makes it particularly suitable for wearable and monitoring applications. When mounted on a dielectric substrate, these antennas become even more practical and effective for integration into wearable technology.

As shown in Fig. (1.10) the bow tie geometry consists of two triangular elements arranged in a symmetrical configuration, resembling the shape of a bow tie. The two elements are usually fed at the center of their bases, where they connect to the transmission line or feed network.

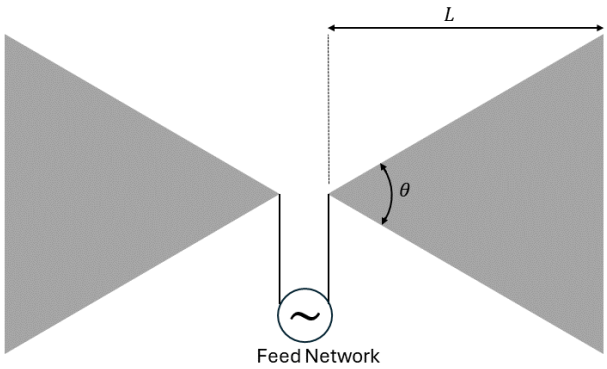

Fig 1.10: Geometry of a Bow tie antenna

The antenna structure is completely defined by its flare angle θ which determines the antenna impedance and length L which determines the operation bandwidth.
These relations are based on the following empirical formulas: [7]

$$L = \frac{1}{2}\lambda_0 \times \frac{1}{\sqrt{\varepsilon_{eff}}} \qquad [1\text{-}40]$$

Where λ_0 is the wave length in the air and ε_{eff} is the effective dielectric constant which can be obtained by:

$$\varepsilon_{eff} = \frac{\varepsilon_r+1}{2} + \frac{\varepsilon_r-1}{2}\left(1 + 10\frac{h}{w}\right)^{-0.555} \qquad [1\text{-}41]$$

Where ε_r is the dielctric constant of the substrate, h is the thickness of the substrate and w is the width of the feeding microstrip.
The flare angle θ and the antenna impedance Z_{in} are related by: (Biconical approximation method) [8]:

$$Z_{in} = 120\ ln\left[\cot\frac{\theta}{4}\right] \qquad [1\text{-}42]$$

The radiation pattern of this antenna is very similar to the one of the dipole antenna, it has a bidirectional pattern with broad main lobes perpendicular to the plan of the antenna as shown in Fig. (1.11). The antenna is linearly polarized; with maximum radiation at 90 degrees to the antenna's axis.

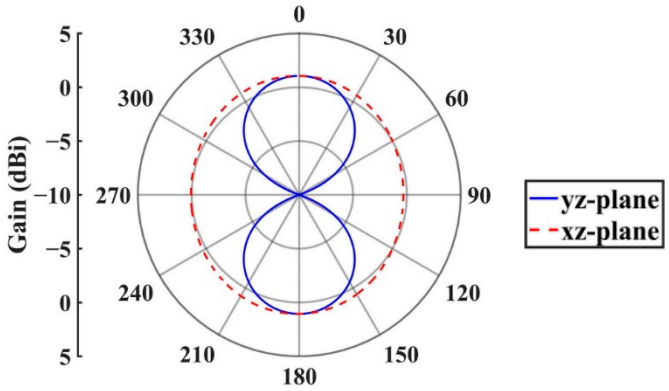

Fig 1.11: Radiation pattern (Gain) of a bow tie antenna at 400 MHz

FRACTAL BOW-TIE ANTENNA

Fractal antennas are a thoroughly researched class of antennas that implement fractal geometry to achieve unique performance characteristics. Fractal geometry involves shapes that exhibit self-similarity, meaning that the same shape repeats at different scales.

Fractal antennas can operate across multiple frequency bands or over a wide frequency range because their self-similar geometry enables them to resonate at harmonic frequencies, providing multiband or wideband coverage without the need for additional tuning elements.[9]

They also often exhibit improved radiation properties, including higher gain, better impedance matching, and more uniform radiation patterns.

Fractal antennas tend to be more robust to manufacturing imperfections compared to traditional antennas, the self-similar nature of fractal geometry means that minor variations in the fabrication process are less likely to significantly affect the antenna’s performance.

The multiband or wideband characteristics of fractal antennas make them suitable for frequency-agile and reconfigurable systems. By adjusting the operating frequency or changing the fractal geometry, the antenna's performance can be optimized for different communication requirements.

The Sierpiński triangle is one of the most used geometries in the antenna field as well as other variations [10] [11] .

This fractal was created by the Polish mathematician Waclaw Sierpinski and is obtained by dividing the initiator (an equilateral triangle) into four equilateral triangles, removing the central one (level 1). By repeating the process on the remaining triangles, the geometry shown in Fig. 1.12 is obtained.

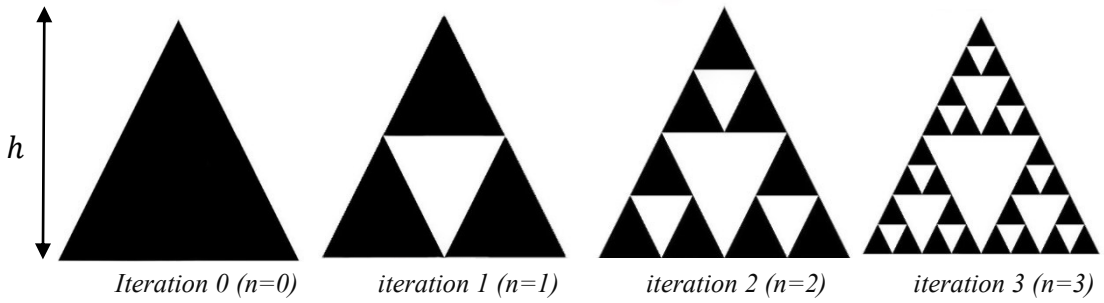

Fig 1.12: Sierpinsky geometry

If h and A_0 are respectively the height and the area of the initiator, then the total height h_n and the total area A_0 of the Sierpinsky triangle are :

$$h_n = 2^n\, h \qquad n = 1,2,\ldots \qquad [1\text{-}43]$$

$$A_n = \left(\frac{3}{4}\right)^n A_0 \qquad n = 1,2,\ldots \qquad [1\text{-}44]$$

where n is the number of the iteration necessary to create the Sierpinky triangle.

Due to its iterative geometry, the antenna presents log-spaced bands depending on how many fractal iterations are included in the geometry.[12] Fig (1.13)

For a Sierpinski monopole antenna each resonant frequency can be calculated as follow [13]:

$$f_n = (\alpha + 0.44k)\,\frac{c}{h}\;2^k \qquad [1\text{-}45]$$

Where c is the speed of light in vacuum, h is the heigh of the largest triangle, k is a natural number and α is a parameter that takes into account the type of substrate the antenna is mounted on.

α =0.194 for thinner substrates [14]

α =0.17 for thicker substrates [13]

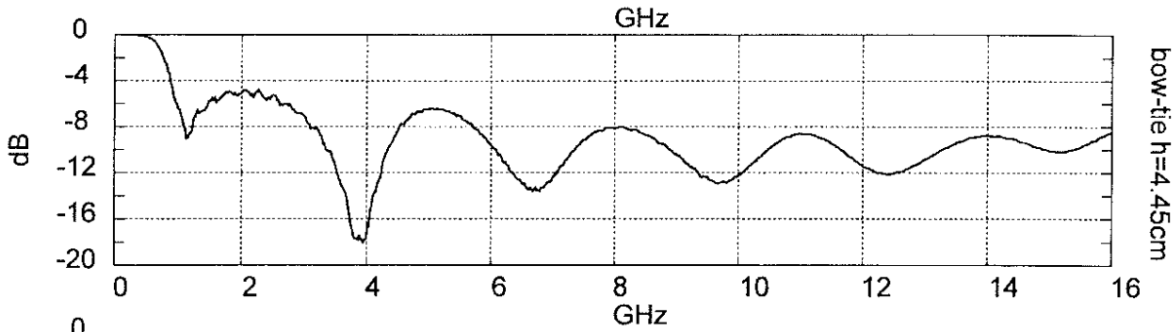

Fig. 1.13: S11 of a fractal bow-tie antenna with arm length of 4.45 cm.

It is also interesting to notice that the similarity and periodicity are lost in the lower bands. This fact is related to the antenna truncation since the structure is not an ideal fractal constructed after an infinite number of iterations.

2

Wearable Antennas

2.1 WEARABLE SYSTEM

Wearable technologies are defined as all types of devices worn on the body, including smart clothing like e-textiles and interactive accessories. The term “wearable computer” covers a wider range of devices and usage concepts. These devices, which include garments and accessories, can sense, process, and interpret user data to offer relevant information, services, and resources.

Regarding digital solutions, the earliest documented example of an interactive wearable device dates back to 1955, credited to Edward Thorp and Steve Channon. They developed a wearable system that aim to predict the trajectory of roulette balls in casinos, which was followed by a device known as a “gambling shoe” [15].

Thanks to the recent advances in micro and nanotechnology, the evolution of wearable technology has progressed not only in terms of hardware, with advancements in the miniaturization of components, but also in the development of more efficient batteries, in the invention of different sensors, and in the emergence of flexible electronics. These innovations allowed wearables to become more lightweight, durable, and capable of being integrated seamlessly into everyday clothing and accessories. As a result, wearable devices have expanded beyond their initial applications in niche markets such as health monitoring and fitness tracking. They now incorporate a broader range of functionalities across various industries, including healthcare, sports, entertainment, and even industrial sectors.

In general, a wearable system is capable of bidirectional data transmission. This means it can collect data from its sensors and transmit or receive information from external sources and take action accordingly. In the first scenario, sensor signals travel through a flexible data bus integrated into the system to a multifunction processor. This controller processes the signals and

wirelessly transmits them using suitable communication protocols such as LoRa, Wi-Fi, or Bluetooth, to designated destinations like a doctor's office or military station.

Sensors play a crucial role in wearable technology by measuring various physical properties of the environment or the wearer, generating signals processed by algorithms. Different types of sensors are employed for specific purposes: acceleration sensors track user's activity and movements, GPS sensors determine location, temperature sensors provide environmental heat levels, while EMG sensors detect small electrical potentials produced during muscle activation. [16]

Noninvasive physiological sensors are widely used in applications such as home healthcare and monitoring individuals, tracking vital signs such as heart rate, movement via accelerometers, and skin surface temperature.

Depending on the goal of the wearable application, the sampling rate for data collection will vary accordingly. Continuous data collection is necessary for certain types of applications, such as heart rate or body temperature, while other applications may require discrete data collection, such as tracking hours of sleep. The decision on sampling frequency involves a trade-off between preserving battery life, and managing storage capacity while also ensuring that the collected data provide meaningful and reliable insights. It's crucial to select a sampling frequency that allows the data to be interpreted accurately and provide valid information about ongoing trends. This means choosing a frequency that captures enough data points to establish reliable patterns and trends, ensuring the data's integrity and usefulness in analysis. For example, to preserve battery power, developers might opt to record location information every five minutes. Alternatively, due to privacy considerations, location data might only be collected during specific times. [17]

The specific features of wearable technology depend on the application goal and domain. Since wearables are worn on the body, their primary application is often in healthcare, where they can continuously monitor vital signs, track activity levels, and provide real-time health data to users and healthcare professionals alike. However, the benefits of wearable technology extend far beyond healthcare. In industrial settings, wearable sensors enhance worker safety by monitoring environmental conditions and detecting hazards in real time. [18]

Moreover, in augmented reality applications, wearable devices integrate digital information with the physical world, offering enhanced visualization and interaction capabilities. These examples underscore the versatility of wearable technology across various sectors, highlighting its potential to revolutionize how we live, work, and play.

2.2 TEXTILE ANTENNAS

In wearable devices, to transmit sensed data wirelessly, an antenna is essential. This antenna must be integrated into the wearable system, often embedded within fabrics or clothing. Hence, the development of textile antennas becomes crucial.

A textile antenna differs from the traditional solid antenna in its construction and materials. Unlike traditional antennas made from rigid materials, textile antennas are partially or entirely fabricated using textile materials, making them more flexible. They typically consist of two types of fabrics: conductive fabrics for conducting patches and non-conductive fabrics for substrates. The choice of fabric influences the antenna's characteristics such as gain, bandwidth, efficiency, and reflection coefficient, which vary based on the substrate's dielectric constant. This flexibility and adaptability of textile antennas allow them to be seamlessly integrated into clothing and textiles, offering unique advantages in wearable technology and other applications where flexibility and comfort are necessary. Most textile antennas are microstrip or patch antennas, chosen for their small size and suitability for various applications such as aerospace, military equipment, and communication devices. Their compact design makes them ideal for applications where space is limited and where seamless integration into clothing or wearable devices is essential for optimal performance. [19]

The advantages of textile antennas can be summarized as follows:

- Comfort and Discreteness: Textile antennas are soft and flexible, ensuring wearer comfort when integrated into clothing. Unlike traditional metallic antennas, they do not cause discomfort or hinder movement. Studies often focus on bending conditions to assess how repetitive bending can potentially degrade the antenna and how different types and directions of bending affect antenna performance.
- Aesthetics: Textile antennas are inconspicuous and can be designed to match the pattern or color of the fabric they are integrated into, enhancing the overall aesthetic appeal of wearable devices.
- Durability: These antennas are engineered to endure the demands of daily wear and washing cycles, maintaining their functionality and performance over an extended period. Studies often investigate how multiple washing cycles affect antenna performance and reliability.

- Customization: Textile antennas can be customized to fit specific shapes and sizes, offering flexibility in their design. This customization capability allows for seamless integration into various types of clothing and accessories, enhancing both functionality and user experience.

2.3 FABRICATION TECHNIQUES

Fabrication methods are pivotal in determining both the speed and accuracy of developing low-cost wearable antenna prototypes. While the choice of materials, whether conductive or non-conductive, is influential, the fabrication techniques themselves also significantly impact the antenna performance.

There are several fabrication processes available that ensure flexibility, low cost, and other desirable characteristics for wearable antennas. Techniques such as inkjet printing, screen printing, embroidery, and even weaving conductive threads into textiles are commonly used. These methods not only facilitate the integration of antennas into flexible substrates like fabrics but also maintain their functionality and durability. By choosing the right fabrication process, designers can achieve antennas that are lightweight, comfortable to wear, and suitable for various applications in wearable technology. Each method offers unique advantages in terms of cost-effectiveness, ease of production, and the ability to adapt to different design requirements, ensuring that wearable antennas meet both technical and practical needs.

FLEXIBLE ADHESIVE CONDUCTIVE LAYER

A common method involves applying a thin and uniform metallization layer onto non-conductive textile substrates. This can be achieved by attaching copper or silver tape, or by applying metal foils directly onto the textile fabric. The thickness of the metallization layer significantly influences the antenna's performance, affecting the electrical properties of the antenna such as impedance and radiation efficiency.

Compared to more complex methods like knitting conductive yarns, this approach is relatively simple and quick. However, for mass production of textile antennas, this technique can be slower

due to the manual labor involved. It is suitable for experimental antenna prototyping but may not be ideal for long-term solutions due to potential issues like easy detachment during bending or exposure to environmental conditions. Therefore, while convenient for initial prototypes, careful consideration is necessary for applications requiring durability and scalability.

Another problem with this method is that it can result in significant dimensional errors if the conductive foil is hand-cut. To address this, cutting machines are used to achieve precise dimensions for the antenna structure. After cutting, the conductive textile is attached to a substrate material using a press steamer to ensure a strong bond with the fabric and to minimize any air gaps between the substrate and the conductive textile. [20]

Fig 2.1: Patch antenna with copper conductive foil

INJECT AND SCREEN PRINTING

Inkjet and screen printing methods both involve applying conductive ink onto non-conductive fabric to create the conductive element of the antenna.

Screen printing requires a reusable mask for each antenna design, which can be time-consuming and impractical for individual antennas or when studying antenna geometries. In contrast, inkjet printing does not need a mask but tends to be more time-consuming and expensive.

Common electrically conductive inks available on the market include those made from carbon nanotubes, polymers, and metallic nanoparticles. [21]

However, textiles are often considered less optimal as printing substrates compared to materials such as paper or Kapton. The inherent porosity of fabrics poses a significant challenge during printing, making it difficult to achieve continuous, reliable conducting lines. This issue can result in inconsistencies in the deposition of conductive ink, impacting the overall performance and durability of printed electronic components, including antennas. The durability of the antenna can be enhanced by either adding multiple layers of conducting ink or applying a TPU (thermoplastic polyurethane) lamination on top. These methods improve washability and protect against wear. However, adding multiple layers can result in less defined edges, potentially affecting the antenna's performance and aesthetic appearance. [22]
Therefore, achieving a balance between durability and maintaining sharp, precise antenna features is crucial in the design and fabrication process.

EMBRODERING

Embroidered textile antennas are a type of wearable antenna integrated into fabric through embroidery techniques. These antennas are manufactured by stitching conductive threads onto a textile substrate, creating a customized antenna pattern. To fabricate these antennas, a common embroidery machine is used. These machines, typically employed for standard sewing and embroidery purposes, operate using two threads: the upper thread and the bobbin thread. For applications in textile electronics, the first one is a conductive thread while the second one is a normal non-conductive thread, most commonly cotton. While the basic principles remain the same, advancements in technology now allow for digital images to be directly embroidered using computer-aided embroidery machines (Figure 2.2). The conductive threads used must be flexible and strong enough to endure the high tensions applied by the embroidery machine without breaking.

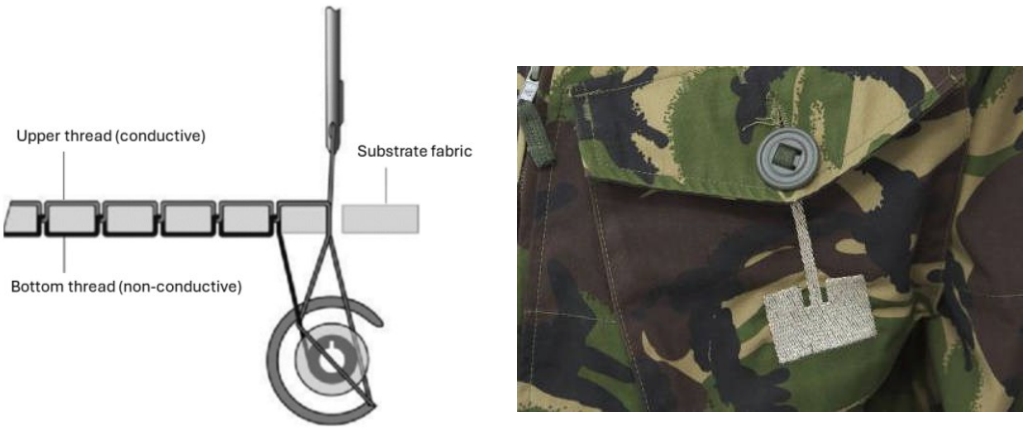

a) *b)*

Fig 2.2: a) Machine embroidering technique b) Example of a Textile antenna on clothing

When embarking on embroidery, several critical decisions come into play. Initially, the choice of conductive thread; its composition and dimensions significantly influences antenna performance. Next, considerations such as stitch direction (optimal efficiency often aligns with the direction of current flow), stitch spacing, and whether to use single or multiple layers, all play pivotal roles in the process [22]. These choices collectively shape the effectiveness and functionality of the embroidered antenna.

Moreover, simulating the exact behavior of an embroidered antenna, including the stitching pattern, using simulation tools is extremely difficult. This complexity underscores the necessity of physical prototyping to accurately assess how an antenna will perform in real-world conditions. Physical testing remains indispensable for validating antenna performance and optimizing design parameters effectively.

Embroidery offers several advantages over other manufacturing techniques, mainly because embroidery machines are already well-established in the industry. This facilitates the mass production of garments integrated with embroidered textile antennas. In embroidered antennas, currents flow more smoothly along threads rather then from threads to threads, making linear antenna designs like dipoles or spirals easier to implement compared to methods using copper tape.

Similar to other techniques, embroidery's cost efficiency depends significantly on minimizing material wastage during production.

Embroidery is particularly adept at creating complex geometries thanks to computerized machines. Although embroidery's accuracy is generally limited to around one millimeter, advancements in computer-aided techniques can enhance precision.
Moreover, unlike some other methods, embroidery often eliminates the need for glue to bond textile layers, which improves the washability and durability of garments with integrated antennas. This makes embroidery a versatile and attractive option for designing wearable textile antennas, offering both efficiency and flexibility in mass production.

KNITTING AND WEAVING

Many applications have been developed using textile antennas created with woven or knitted conductive sheets.
When employing weaving techniques, the yarns are interlaced horizontally and vertically to create a flat and dense structure. This involves two sets of yarns crossing each other to form a grid-like pattern. On the other hand, in knitting, the threads run parallel and form interconnected loops, which can be arranged in various patterns and densities. This loop structure makes knitted fabrics more elastic, as the threads follow one another in each row, allowing for greater stretch and flexibility compared to the more rigid woven fabrics.
In some applications, the fabric is first knitted or woven using non-conductive yarns, such as fleece or woven material, and then it is plated with a conductive material like Nickel or Copper. This process transforms the originally non-conductive fabric into a conductive one [23].
There are several methods to attach the conductive sheet to the substrate fabric:

- Sawing
- Liquid textile adhesive (golden fix)
- Adhesive sheets that melt when ironed

The third attachment method produced the best results. It had a negligible effect on the thickness of the substrate, allowing the antenna to keep its intended geometrical dimensions.

Fig 2.3: Knitted dipole antenna

2.4 SUBSTRATE MATERIAL SELECTION

Choosing the appropriate dielectric substrate for a textile antenna is a critical step that influences the overall performance of the antenna. The dielectric substrate must have certain key properties, including flexibility, durability, and compatibility with conductive materials. Additionally, the substrate must have minimal impact on the antenna's electrical characteristics, such as permittivity and loss tangent, to ensure optimal performance.

The permittivity ε of a material is defined as in [1-8] and the relative value ε_r is a complex number:

$$\varepsilon_r = \varepsilon' - j\varepsilon'' \qquad [2\text{-}1]$$

The imaginary part ε'' describes the energy loss within a dielectric material. The dielectric loss tangent tan δ is defined as the ratio of the imaginary part ε'' to the real part ε' of the relative dielectric constant ε_r. Ideally, a perfect dielectric material has tan δ = 0, indicating no energy loss.

$$\text{Tan}\,\delta = \frac{\varepsilon''}{\varepsilon'} \qquad [2\text{-}2]$$

In general, dielectric properties are influenced by factors such as frequency, temperature, surface roughness, moisture content, purity, and material homogeneity. For isotropic media under constant temperature and frequency of electric field, the relative permittivity ε_r remains a static scalar value. However, textiles are anisotropic materials, meaning their properties vary with the orientation of the electric field. This directional dependency is fully characterized by a second-order permittivity tensor, though often a single component of this tensor is sufficient.

Commercially available textiles are typically highly porous, resulting in a low relative permittivity $\varepsilon_r < 2$. This low ε_r helps reduce surface wave losses associated with guided wave propagation within the substrates. As a result, spatial wave propagation and impedance bandwidth of antennas can increase, facilitating the development of antennas with high efficiency and gain.

In Tab 2.1 are shown the dielectric properties of the most common dielectric materials used as antenna substrates.

Dielectric material	Dielectric constant ε_r	Loss tangent $tan\,\delta$
Cotton	1.6	0.0400
Silk	1.75	0.012
Felt	1.22	0.016
Lycra	1.50	0.0093
100% Polyester	1.90	0.0045
Jeans	1.70	0.025

Tab 2.1: Dielectric properties of non-conductive fabrics

Accurately determining the dielectric properties of these materials remains a challenge. Woven, knitted, and nonwoven fabrics exhibit inherent inhomogeneity and high porosity, making them susceptible to fluctuations in environmental conditions. This complicates the electromagnetic characterization of textile materials. There are several methods to carefully measure a material's permittivity.

The *Cavity Perturbation Method* is often used for measuring materials with moderate to low losses. This technique employs closed cavities, typically cylindrical or rectangular in shape. A cavity without any sample has a specific resonant frequency. When a dielectric sample is introduced into the cavity, this resonant frequency shifts, allowing for the determination of the dielectric properties of the material [24].

In the *Transmission Line Method*, the material under test is placed inside either a coaxial air cell or a waveguide cell. A probe connected to a vector network analyzer (VNA) measures the complex scattering parameters at both ports. Different methods are available to calculate the dielectric constant from the S-parameters [25].

The thickness of the dielectric substrate also plays a crucial role, it mainly characterizes the gain, bandwidth, and radiation efficiency of an antenna.

The emphasis is on maximizing radiated power, which typically results in a low quality factor Q. For thin substrates ($h \ll \gamma_0$), the quality factor is primarily influenced by radiation efficiency Q_{rad}. Since Q_{rad} decreases with thinner substrates, it becomes beneficial to use thicker substrates. This is because Q_{rad} is inversely proportional to the height of the substrate, meaning a thicker substrate can improve the antenna's overall performance.

However, it is shown that a thicker material results in larger surface waves which is undesirable because it reduces the radiation efficiency. [26]

The goal is to find a good match between substrate height and surface wave losses. Usually, a good choice for the substrate thickness is between 0.003λ and 0.005λ. [27]

2.5 CONDUCTIVE MATERIAL SELECTION

The choice of conductive material for the antenna's patch is crucial, alongside the substrate's thickness and dielectric constant

Since textile antennas are planar structures, they are characterized by their electrical behavior through metrics like surface resistance and resistivity (Ω m). To ensure minimal electrical losses and maximize antenna efficiency, it is important to maintain a low and stable surface resistance. Commercially available conductive textiles typically exhibit surface electrical resistance below 1 Ω/m, a measure applicable to materials with uniform thickness.

The conductivity σ is related to the surface resistivity ρ_s through:

$$\sigma = \frac{1}{\rho_s \, t} \quad \left[\frac{S}{m}\right] \qquad [2\text{-}3]$$

Where t describes the thickness of the material.

Threads coated with conductive materials or containing conductive wires serve as the foundational component, enabling the creation of wash-resistant, flexible, and stretchable fabric.

In the context of textile antennas, options for conductive yarn include metalized polymer yarns, conductive hybrid yarns, or conductive polymer threads.

Conductive hybrid threads are combinations of ultra-fine metal wires, typically made from stainless steel, copper, brass, nickel, or iron alloys, with synthetic threads such as polyester (PES) or polyamide (PA).

The main difference in these hybrid yarns lies in the number of conductive wires within the thread and their respective diameters. These factors vary depending on the specific application area and dictate the use of the conductive material. Together, they significantly influence the electrical properties of the yarn, particularly the electrical linear resistance, which tends to be very low when using conductive hybrid threads.

For example, CleverTex, twists metallic microwires (copper and Silver plated) with a non-conductive high-strength PES thread (Fig. 2.4). A multifunctional smart yarn is the result of this process. It is fully compatible with known textile technology processes such as sewing, embroidery, weaving or knitting.

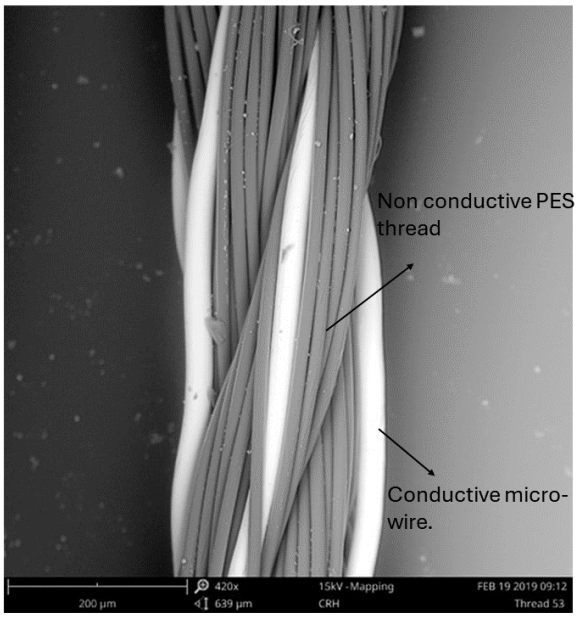

Fig 2.4 Conductive hybrid thread

Material Composition	No. of synthetic threads	No. of metal wires	Diameter [mm]	Linear resistance $[\Omega/m]$
PES multifil/ Cu Ag	4	4	0.23	6.5
PES multifil/ Cu Ag (insulated)	2	8	0.18	3.0
Elastil multifil/ Cu Ag	2	8	0.21	3.2
Silver coated Polyamide/ Polyester	1	2	0.40	<85

Tab 2.2: Overview of the material parameters of the most common hybrid conductive yarns

When the antenna patch directly contacts the skin, insulated wires are often chosen to prevent skin irritation from metal contact. However, considerations about ensuring reliable electrical contact and maintaining insulation integrity must be taken. Ongoing research focuses on developing textile wire insulation, with thermoplastics and other materials. Importantly, the insulation process does not compromise the mechanical or electrical properties of the final textile filaments. [27]

2.6 ANTENNA DESIGN CHALLENGES

Designing antennas for wearable applications presents several unique challenges due to the integration of electronic components with flexible and often non-conventional substrates. These challenges goes from the need to maintain antenna performance while ensuring comfort, durability, and aesthetic appeal.

They must be able to withstand bending, stretching, and washing cycles without compromising performance. The antenna material and substrate must be selected or engineered to maintain mechanical integrity under these conditions.

Antennas need to be seamlessly integrated into textiles, which are typically non-conductive and flexible. Techniques such as embroidery, printing (screen printing or inkjet printing), weaving conductive fibers, or using conductive textiles are employed to achieve this integration while

maintaining functionality. If the fabrication process involves the use of conductive thread the first step is to select the most suitable yarn in terms of conductivity, strength, flexibility; then it's important to investigate its behavior when it's stitched to form an approximately continuous object in order to improve the efficiency of the patch antenna. The understanding of the current flow on a designed patch antenna is a fundamental requirement to choose the stitch pattern.
The size and shape of the antenna are constrained by the design requirements of the wearable device and the available area on the textile.

It's possible to have more intricate shapes compared to rigid antennas since their flexibility enables antennas to conform better to the contours of the wearable item. However, several challenges arise in the manufacturing process, particularly when employing techniques like embroidery and knitting. Some margin for error during fabrication must be taken into account. Such techniques require precise control over stitching, thread tension, and material properties. Factors like the capabilities of embroidery machines, the size of needles and yarn, and the resolution of knitting patterns must all be carefully considered. These constraints influence the achievable antenna design complexity and the overall performance of the antenna.
Miniaturization techniques are often necessary to fit antennas within small spaces without sacrificing performance.
Wearable antennas are exposed to various environmental conditions such as moisture, sweat, and temperature fluctuations. Designers must consider these factors to ensure antenna reliability and longevity in real-world applications.
Measurements should be conducted either on a real human body or using a human. These measurements involve assessing parameters such as S11 (reflection coefficient), near-field characteristics, and far-field radiation patterns. It's important to thoroughly characterize how the antenna interacts with the body or phantom to understand its real-world performance.
Measurements can also be performed in controlled environments like an anechoic chamber, which provides isolation from external interference or in real-world environments such as outdoors or indoors, reflecting typical usage scenarios.
Conducting measurements of wearable antennas is not always straightforward due to the characteristics of the materials and the integration with textiles. Flexible materials often have lower conductivity than traditional metals like copper. This difference affects how efficiently the antenna radiates and receives signals.

Additionally, the dielectric properties of the fabric substrate are not always well known and they can vary significantly between suppliers or even different batches from the same supplier. This variation is influenced by factors like the density of fibers within the substrate, which can change within the same material.

Another challenge concerns the substrate thickness, which can change based on how components are attached. Methods like applying adhesive can be inconsistent, making it difficult to maintain uniformity across the substrate.

Also, the connection point between the antenna and its connector is sensitive in wearable antennas. It depends on the antenna's specific position, the orientation relative to the wearer's body and it's not always stable. This variability adds complexity to ensuring reliable and repeatable measurements of antenna performance.

All these factors contribute to the issue of measurement repeatability and consistency. Different prototypes or even repeated measurements of the same prototype can yield slightly different results due to these material and integration variances. This underscores the importance for designers to standardize their projects rigorously and conduct multiple measurements under various conditions to thoroughly study antenna behavior.

2.7 HUMAN BODY INTERACTION

When antennas are placed in direct contact with the human body, the body absorbs and reflects some of the electromagnetic energy. This causes two main effects: first, the presence of human tissue can significantly affect the antenna's performance due to absorption and reflection of electromagnetic energy. Second, the antenna can also impact human tissue, as the body acts like an additional material that alters the antenna's characteristics.

EFFECT OF THE ANTENNA ON THE HUMAN BODY:

Non-ionizing radiations, such as RF waves and microwaves, possess enough energy to move atoms and molecules or cause them to oscillate or vibrate. They can then set in motion molecules and raise the material temperature, impacting human tissues. The most common effect of this type is dielectric heating, which occurs when the electromagnetic field induces rotations of polar molecules (like that of water that constitutes the largest part of human tissues), heating the

dielectric material. If these effects impact the skin tissue where the antenna is placed, it raises a series of potential concerns and effects on the human body that need to be carefully evaluated and given attention.

The parameter that is used to measure the rate at which energy is absorbed by human tissues is the Specific Absorption Rate (SAR):

$$SAR = \frac{\sigma |E|^2}{\rho} \quad \left[\frac{W}{Kg}\right] \qquad [2\text{-}4]$$

Where σ is the conductivity of the tissue, ρ is the mass density of the tissue and E is the rms electric field strength.

There are different SAR values depending on the volume and type of tissue considered and the context of the measurement.

The Whole-Body SAR measures the average energy absorption rate over the entire body. It provides an overall assessment of the total energy absorbed by the body and is used to evaluate the safety of exposure to large, uniform fields, such as those from environmental sources or whole-body scanners.

The Localized SAR measures the energy absorption rate in a specific, smaller mass of tissue. Commonly, localized SAR is assessed in volumes of 1 gr. or 10 gr. of tissue. This measurement is relevant for identifying areas with higher energy absorption that could lead to localized heating and potential thermal damage. For example, in the case of devices like mobile phones, where the antenna is close to a specific body part, such as the head.

There are various rules and regulations in the world regarding the SAR limit of electromagnetic devices. In the United States the Federal Communication Commission (FCC) has established the SAR limit to 1.6 W/kg averaged over 1 gr. of actual tissue, while the Council of European Union has fixed the limit to 2 W/kg averaged over 10 gr. of actual tissue. In the case of head exposure, it corresponds to imposing a limit of temperature increase in the head tissues of 1 K. [28]

EFFECT OF THE HUMAN BODY ON THE ANTENNA:

When a wearable antenna is close to the human body, the body's lossy and high dielectric constant characteristics can affect the antenna's performance. This can cause changes in input impedance, frequency shifts, and reduced efficiency, disrupting communication with external

devices. The placement and orientation of the antenna, as well as its distance from the body, are crucial in minimizing these effects.

To evaluate the impact on the human body, simulations are often conducted using software that includes human body models. Additionally, real phantoms made from materials that mimic human tissue are used to study and optimize antenna performance in realistic conditions.

Soft tissues have a high dielectric constant, typically ranging from 20 to 50. This characteristic causes dielectric loading, which shifts the antenna's resonant frequency when it's nearby.

The impact of the human body on antenna performance manifests in two primary ways:

- Reduction in Efficiency: The proximity of the antenna to the body leads to significant absorption of electromagnetic waves. This absorption reduces the antenna's efficiency in radiating electromagnetic energy into free space.
- Changes in Input impedance: If the user is too close to the antenna, the body's presence alters the antenna's input impedance. This alteration can lower the antenna's performance by mismatching with the transmitter or receiver electronics.

To assess these effects, two key metrics are commonly used. The *Body-Induced Gain* compares the antenna's gain when worn on the body to its gain in free space, typically measured in decibels (dB) and the *Body-Worn Efficiency* quantifies the ratio of the total radiated power when the antenna is worn on the body to the total radiated power in free space. [29]

3

Design methodology and experimental evaluation

3.1 PROJECT DESCRIPTION

This work presents a stand-alone wearable system able to monitor the body temperature of the wearer in real-time with a compact and adaptable design. The setup is tailored to be easily assembled by regular users, ensuring accessibility for young students interested in exploring technology.
Based on this project, a workshop was conducted in Regensburg Germany; it was a hands-on activity designed exclusively for girls to introduce them to the STEM field and foster their curiosity in science and technology.

The system has three fundamental components:

- A textile embroidered antenna customized to operate within the unlicensed 863-870 MHz band.
- A development board working at a range frequency of 863 – 928 MHz that is capable of transmitting data through LoRa WAN connectivity.
- A probe sensor able to detect body temperature upon direct contact with skin.

The system is easily assembled by regular users because it can be manufactured and put together without any specialized tools. The antenna can be embroidered also by hand using just a needle and thread, and assembling the other components only requires a soldering iron. While the initial creation and design of the system and antenna require expert knowledge, the replication process can be easily performed by non-expert users.

Two different designs of the textile antenna are being employed: a bow-tie antenna based on the Sierpinski fractal and a dipole antenna. Both antenna designs were initially modeled using CST Microwave Studio software package in order to study their behavior and tune the frequency. Afterward, several prototypes were developed until a sample that met the required specifications was achieved.

The progression of the project can be divided into 4 different phases that can be summarized as follows:

PHASE 1: Preliminary Research and Antenna Design Planning

The starting point is the selection of the development board, which determines the frequency at which the antenna needs to be tuned, as well as the dielectric material on which the antenna is going to be embroidered.

With these two parameters, a model of the bow-tie antenna is constructed on CST to determine the appropriate dimensions to start the fabrication process.

This topic will be addressed in Section 3.2.

PHASE 2: Manufacturing process of the embroidered bow-tie antenna

Several prototypes were embroidered, and several changes were necessary to obtain a final sample that could be used on the wearable system. The adjustments involved the feeding method, stitch pattern, design layout, and embroidery machine settings.

This phase of the project, namely the laboratory testing and implementation stage, was conducted in Pilsen, Czech Republic, in the laboratories of the Department of Electronics at the University of West Bohemia.

This topic will be addressed in Section 3.3.

PHASE 3: Manufacturing process of the embroidered dipole antenna

The same process was repeated for the textile dipole antenna. Starting from a CST model several prototypes were embroidered until a final working dipole antenna was obtained.

This topic will be addressed in Section 3.4.

PHASE 4: Device Configuration and Final Implementation

The final step consists of configuring the development board. The Arduino code is tailored to collect the temperature data from the sensor and seamlessly transmit it via LoRaWAN thanks to the textile antenna.

This topic will be addressed in Section 4.3.

3.2 DESIGN AND CST SIMULATIONS

The resonant frequency of the textile antenna is chosen at 868MHz which falls within the unlicensed band spanning from 868 to 915 MHz. The dimensions of the antenna can be computed based on the dielectric constant of the substrate, the thickness of the substrate and by tuning the resonant frequency. For this purpose, a model is created using the CST Microwave Studio to evaluate the performances of both the bow tie and the dipole antenna designs. The goal is to identify the right dimensions, parameters and stitch pattern necessary to obtain a resonant frequency of 868 MHz.

The Sierpinsky fractal bow tie design is presented first.

BOW TIE ANTENNA

The CST model is based on the repetition of a "unit cell" which is an equilateral triangle with a side length equal to 14 mm. Each triangle is filled with parallel lines spaced 0.1 mm apart resembling a sinusoidal shape to simulate the movement of the thread weaving in and out of the fabric. The thread used is a cylinder structure with a radius equal to 0.1 mm made of PEC (Perfect Electric Conductor). The distance between two needle penetrations is 1 mm.

Adding a perimeter to the unit triangle is necessary to feed all thread lines with current. Such perimeter is 0.01 mm thick, 0.3 mm wide and made of PEC.

The substrate is modeled as a rectangular slab made out of cotton. It's 1.5 mm thick 84 mm wide along the x-axis and 56 mm long along the y-axis.

The substrate material was chosen as pure cotton with a relative permittivity of 1.6 and tangent loss of 0.02. The thickness of the dielectric slab was set at 1.5 mm, mirroring the thickness of

the real cotton fabric that is used. The parameters aforementioned are reported in Tables 3.1 and 3.2.

Design parameters	**Value [mm]**
Side length unit triangle (L_tr)	14
Distance between lines	0.1
Wire radius (r)	0.1
Distance needle penetrations	1
Thickness of the perimeter	0.01
Height of the perimeter	0.3
Gap between the 2 sides	1.1
Thickness of the substrate	1.5
X-axis substrate length	84
Y- axis substrate length	56

Tab 3.1: Geometrical and fabrication characteristics of the bow-antenna prototype

Cotton parameters	**Value**
Relative permittivity (ϵ_r)	1.6
Tangent loss ($tan\,\delta$)	0.02

Tab 3.2: Permittivity and Tangent Loss of the Substrate Material

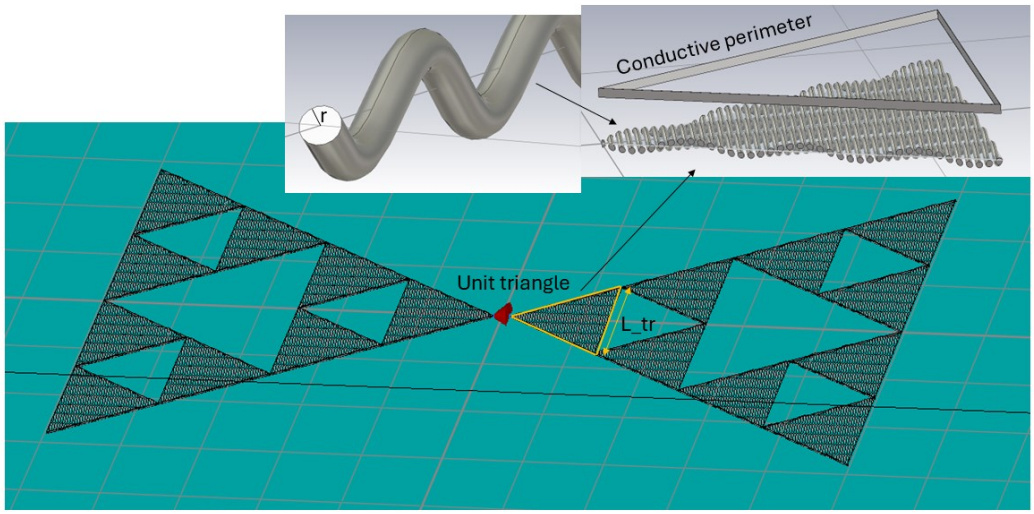

Fig 3.1: CST model embroidered Bow-tie antenna

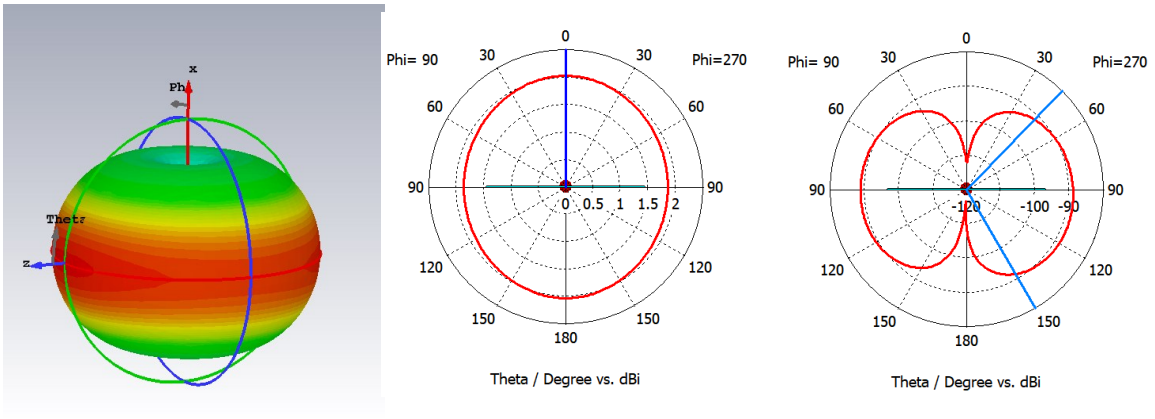

a) *b)* *c)*

Fig 3.2 Bow tie antenna radiation pattern at 868 MHz a) 3D pattern b) Bow-tie Azimuthal plane plot c) Bow-tie Elevation plane plot

The radiation pattern (Fig 3.2) observed for the bow tie antenna in the CST simulation closely resembles that of a traditional dipole antenna, as expected. This similarity arises because the bow tie antenna is essentially a variation of the dipole, featuring a broader bandwidth due to its shape. The radiation pattern is predominantly omnidirectional in the plane perpendicular to the axis of the antenna, exhibiting a doughnut-like shape with maximum radiation occurring in the directions perpendicular to the antenna elements (Fig 3.2a).

Notice from Figure 3.2b that the azimuth plane pattern is omnidirectional, resembling a circular shape that passes through the peak gain at all angles.

From the elevation plane pattern, we see that the antenna has an elevation plane 3 dB beamwidth of 105.4 degrees as indicated on the pattern in Figure 3.2c by the two blue lines.

The two prominent, symmetrical lobes extending outward, show strong radiation perpendicular to the antenna axis and minimal radiation along the axis.

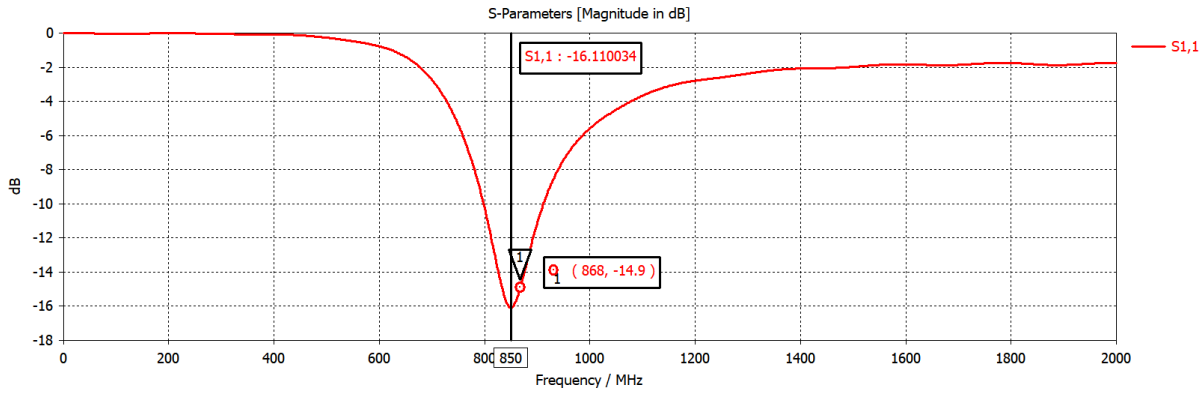

Fig 3.3: Bow-tie antenna S11 parameter

The S11 parameter of the bow tie antenna, which represents the reflection coefficient or return loss, shows a minimum at 850 MHz of 16 dB. (Fig. 3.3)

At the desired operating frequency of 868 MHz, which is close to this peak, the antenna exhibits a RL of 16 dB. Ideally, as a fractal antenna, it should demonstrate multiple peaks at various resonant frequencies, providing wideband performance due to its self-similar structure. However, in the simulation, the model does not exhibit these multiple peaks. This indicates that the antenna behaves more like a traditional, non-fractal bow tie antenna, essentially functioning as an empty wire bow tie antenna.

From Fig. 3.4, it can be noticed that the current is concentrated on the outer perimeter of the bow tie antenna rather than on the triangle element. This observation confirms that the current distribution is primarily along the outer edges, which aligns with the behavior of a conventional non-fractal wire antenna.

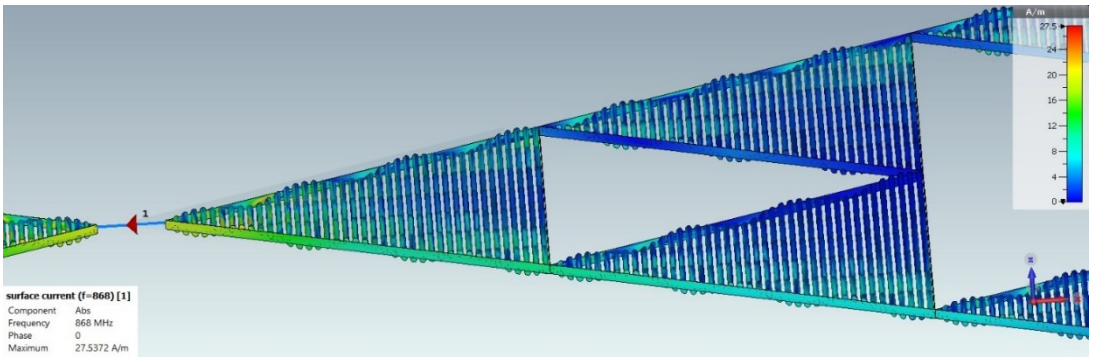

Fig 3.4: Current distribution at 868 MHz

In comparison to the embroidered model of the bow tie antenna with identical dimensions, a patch antenna configuration was also modeled using a solid conductive PEC area. Figure 3.6 illustrates that the patch antenna exhibits a resonant frequency of 916 MHz, which is 66 MHz higher than that of the embroidered model. Additionally, the patch antenna shows a small increase in return loss by 3 dB.

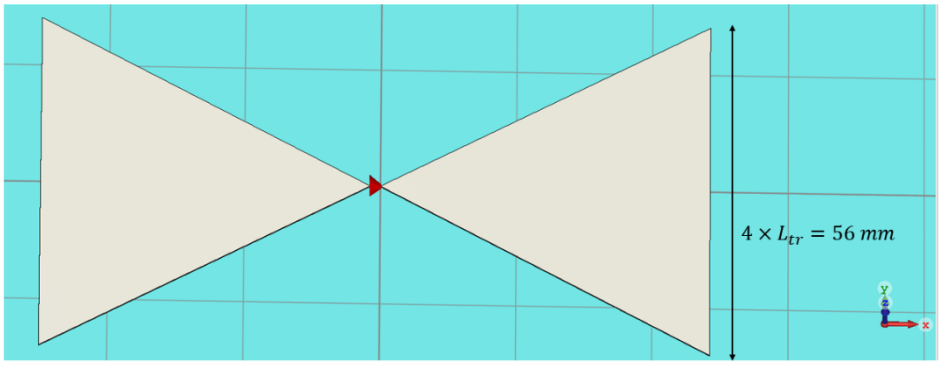

Fig 3.5: CST model patch bow-tie antenna

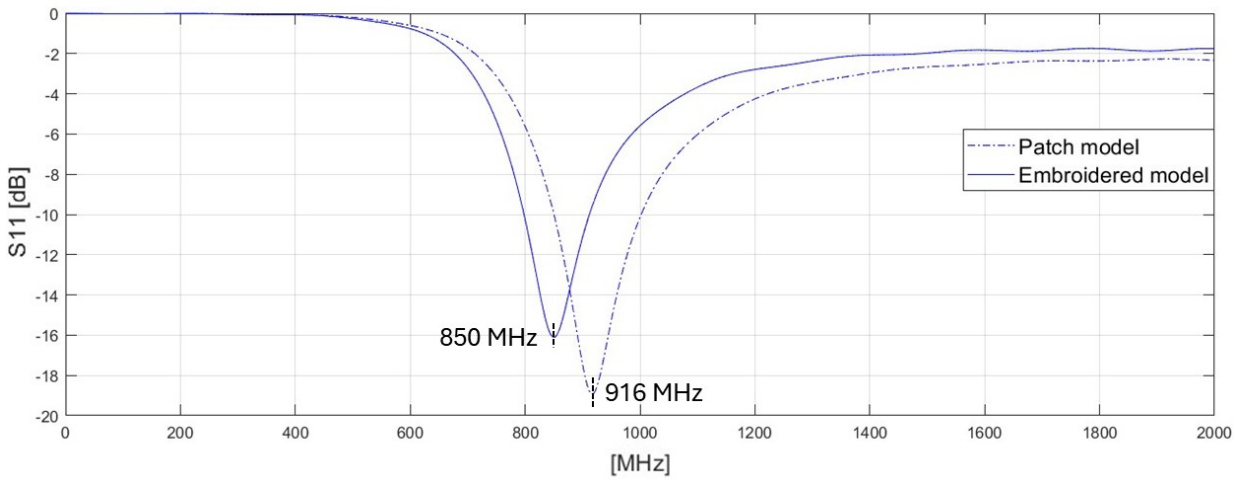

Fig 3.6: S11 of bow-tie antenna: (full) Embroidered model (dotted) Patch model

DIPOLE ANTENNA

The model consists of a half-wave dipole, where the length of the dipole elements is set to half the wavelength of the desired frequency 868 MHz. The theoretical length of the dipole is calculated as follows:

$$L = \frac{c}{2f} = 172mm \qquad [3\text{-}1]$$

This choice of length ensures that the dipole operates at resonance, maximizing its radiation efficiency and achieving optimal impedance matching at the desired frequency.

From [3-1] the calculated optimal length for the half-wave dipole antenna at the desired frequency is 172 mm. However, according to the CST model, this value resulted in a resonant frequency that was too low. To achieve the desired resonant frequency of 868 MHz, the arm length needed to be reduced to 140 mm.

The CST model of the dipole antenna resembles a grid; each line of the grid represents the stitching thread, which is modeled with a PEC cylinder with a radius of 0.1 m. This design made of overlapping lines represents the stitching pattern that is implemented in the real antenna.

To ensure that all thread lines receive current, it's essential to include a perimeter around both arms. The perimeter is constructed with PEC material measuring 0.01 mm in thickness and 0.3 mm in width. The dielectric layer is represented in the same manner as the first model, with a slab of cotton material with a permittivity of 1.6 and tangent loss of 0.02.

The measures of all parameters are listed in Table 3.3.

Design parameters	Value [mm]
Arm length (dL)	140
Second (vertical) arm length (d_p)	10
Gap between two sides (d_s)	5
Width of both arms (d_w)	5
Wire radius (r)	0.1
Distance between lines (d)	1
Thickness perimeter	0.05
Hight perimeter	0.2
Thickness substrate	1.5
X-axis substrate	84
Y- axis substrate	56

Tab 3.3: Geometrical and fabrication characteristics of the dipole antenna prototype

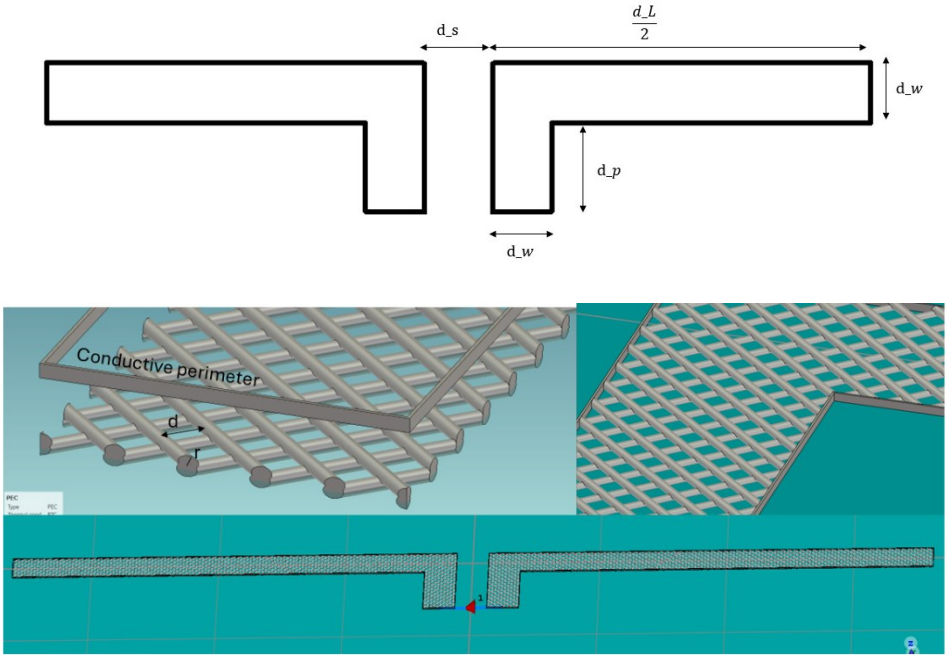

Fig 3.7 CST model dipole antenna

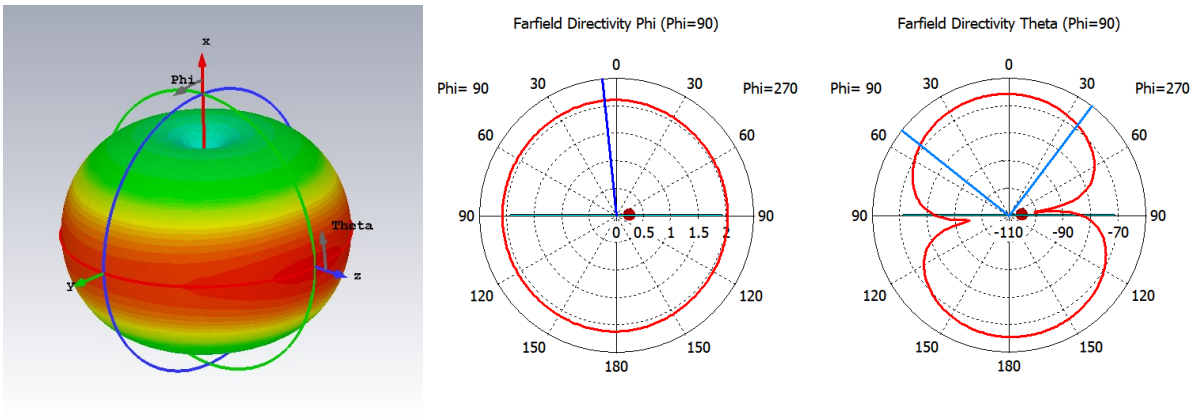

a) *b)* *c)*

Fig 3.8 Dipole antenna radiation pattern at 868 MHz a) 3D pattern b) Azimuthal plane plot c) Elevation plane plot

The simulation results yield the characteristic radiation pattern of a dipole antenna.

The 3D radiation pattern (Fig 3.8.a) shows the expected toroidal shape, with peak radiation in the plane perpendicular to the antenna's axis and minimal radiation along the axis. This pattern indicates efficient radiation in all horizontal directions, forming a doughnut-shaped field.

In the azimuthal plane, the plot displays the typical circular pattern, illustrating the antenna's omnidirectional radiation characteristics around its horizontal axis. (Fig 3.8 b)

In contrast, the polar coordinates plot of the elevation plane reveals two distinct lobes symmetrically positioned around the origin. (Fig 3.8c).

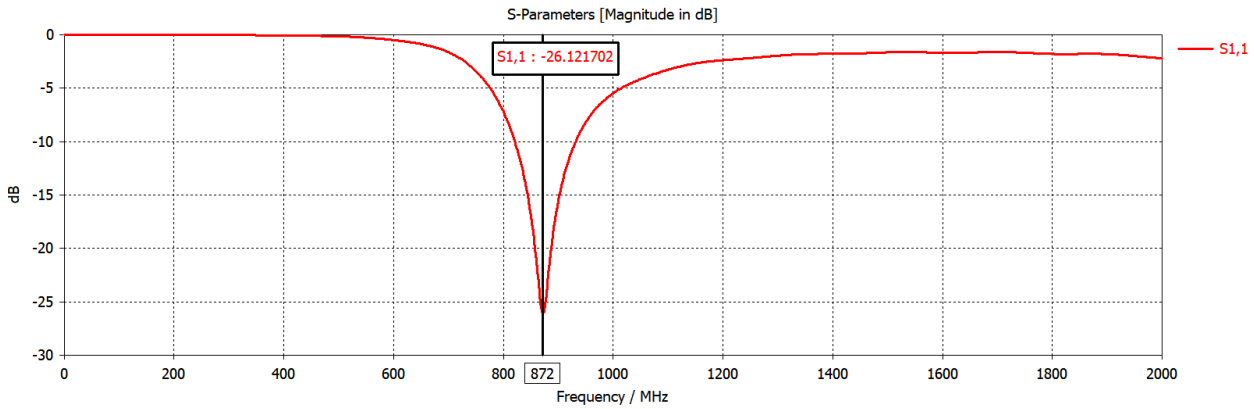

Fig 3.9 Dipole antenna S11 parameter

At a peak frequency of 872 MHz, the dipole antenna exhibits a reflection coefficient corresponding to a RL of 26 dB. At the desired operating frequency of 868 MHz, which is closely aligned with this minimum peak, the antenna demonstrates a similar RL of approximately 25 dB. This suggests that the antenna achieves effective impedance matching at the desired frequency.

3.3 FABRICATION PROCESS: BOW TIE ANTENNA

The manufacturing process involves a series of iterative prototypes and extensive parameter adjustments in order to identify the optimal configuration.
The primary focus lies in centering the resonant frequency at 868 MHz, achieved through targeted adjustments to the following parameters:

- Side length L of the unit triangle
- Density and direction of stitches:
    - High density (HD)
    - Low density (LD)
    - One layer of stitches (1D)
    - Two layers of stitches in opposite directions (2D)
- Type of edges of the unit triangle:
    - Edges embroidered with a “Zig-Zag” type of stitch (ZE)
    - Edges embroidered with a Normal stitch (NE)
- Conduductive thread on one (C1) or both sides (C2)

All the prototypes of the antenna that are presented are embroidered on a pure cotton fabric using the Bernina QE750 sewing machine, equipped with a dedicated module for embroidering. The Bernina offers a wide selection of 837 stitch patterns and is furnished with 70 exclusive embroidery designs [30].
The conductive thread used is a silver hybrid thread which is composed of 4 strands; each one contains 33 polyester (PES) fibers and one silver plated copper microwire (Cu/Ag) (Fig 3.10b). As a non-conductive thread, a common cotton sewing thread is used.

The measurements were conducted for all prototypes in free space, under typical indoor environmental conditions (temperature 25° and humidity 67%).

The S11 parameter measurements were taken by connecting the antenna to a VNA using the RGB20 coaxial cable as shown in Figure 3.10a. The hybrid thread is resilient to high temperatures allowing the use of conventional soldering methods.

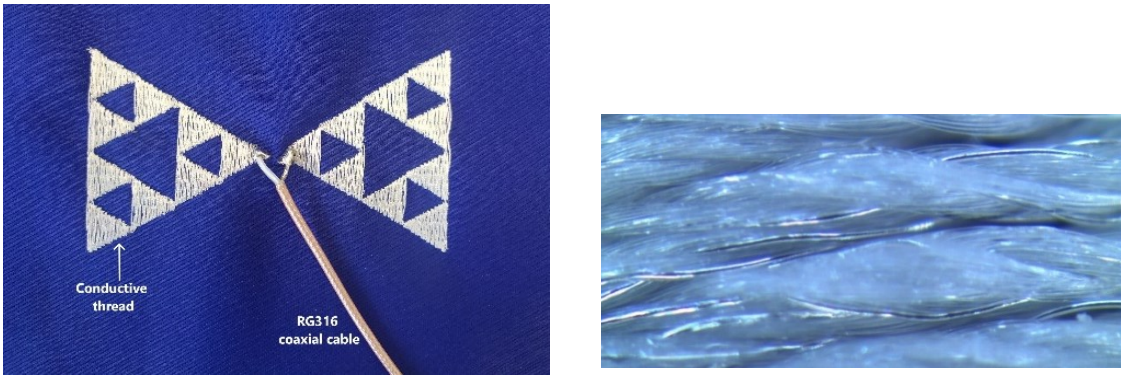

a) *b)*

Fig 3.10: a) Embroidered bow-tie antenna b) Microscope image of the hybrid conductive thread

To maintain consistent stress conditions, the antenna was mounted on a PVC structure for all measurements, ensuring it was not in contact with any surface, which could alter its behavior (particularly important as this antenna is designed for contact with the human body) (Fig 3.11).

Fig 3.11: PVC structure to take measurements

Sample (S)	L_triang [mm]	Stitches direction	Stitches density	Conductive thread	Edges	Freq [MHz]	RL [dB]
2	12	1D	LD	C1	NO	379	13.8
3	14	2D	LD	C1	NO	647	13.19
4	14	2D	HD	C1	NO	650	13.97
5	14	2D	LD	C1	NO	630	16.5
6	12	2D	LD	C1	NO	745	10
7	14	2D	LD	C2	NO	675	16.5
8	10	2D	LD	C1	ZE	1130	29.9
9	10	2D	LD	C1	NE	1095	31.8
10	12	2D	LD	C1	ZE	983	14.5
11	12	2D	LD	C1	NE	988	14.4
12	**14**	**2D**	**LD**	**C1**	**NE**	**864**	**10**

Table 3.4: Summary of the characteristics of the bow-tie antenna prototypes

The resonant frequencies typical of a bow tie fractal antenna are visible in Fig 3.12. The first three resonant frequencies are measured at :

$$f_1 = 248\ MHz$$

$$f_2 = 465\ MHz$$

$$f_3 = 680\ MHz$$

They appear to be evenly spaced, roughly doubling in frequency as [1-45] suggests.

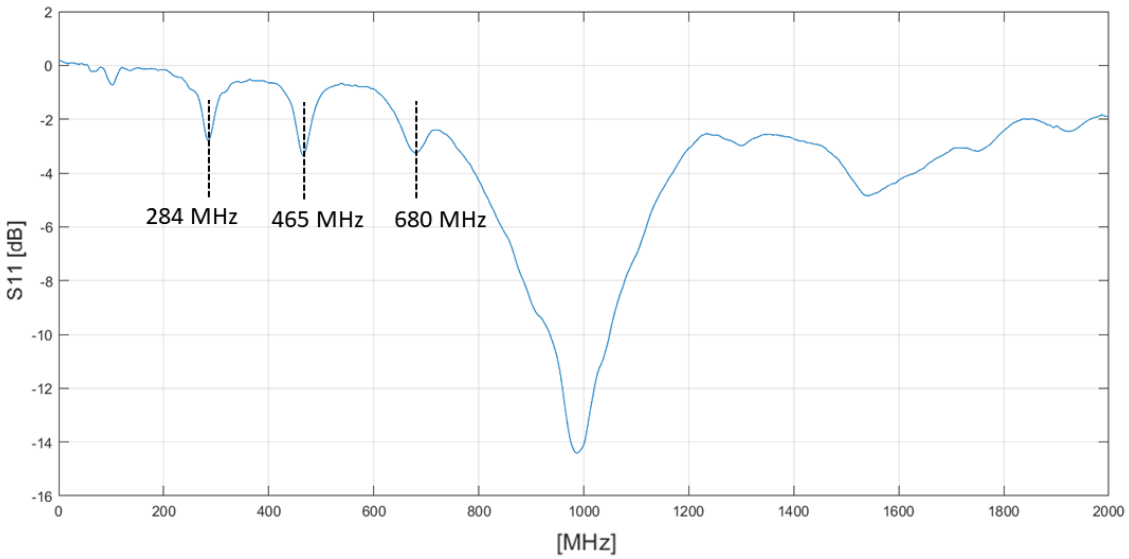

Fig 3.12: S11 of sample 11

Figure 3.13a presents a comparison of the S11 parameter for samples 9, 11 and 12, each featuring a fundamental triangle with lengths L of 10 mm, 11 mm, and 12 mm, respectively. In all three samples, the triangle has edges stitched normally.

Fig 3.13b compares Samples 3 and 6 having L=14 mm and L=12 mm respectively. In both samples, the unit triangle has no edges.

As expected, there's a clear trend where increasing the length of the triangle results in lowering resonant frequencies. This relationship is primarily due to the fundamental principle that the resonant frequency of an antenna is inversely proportional to its physical size. Larger antennas have longer electrical lengths and can support lower resonant frequencies.

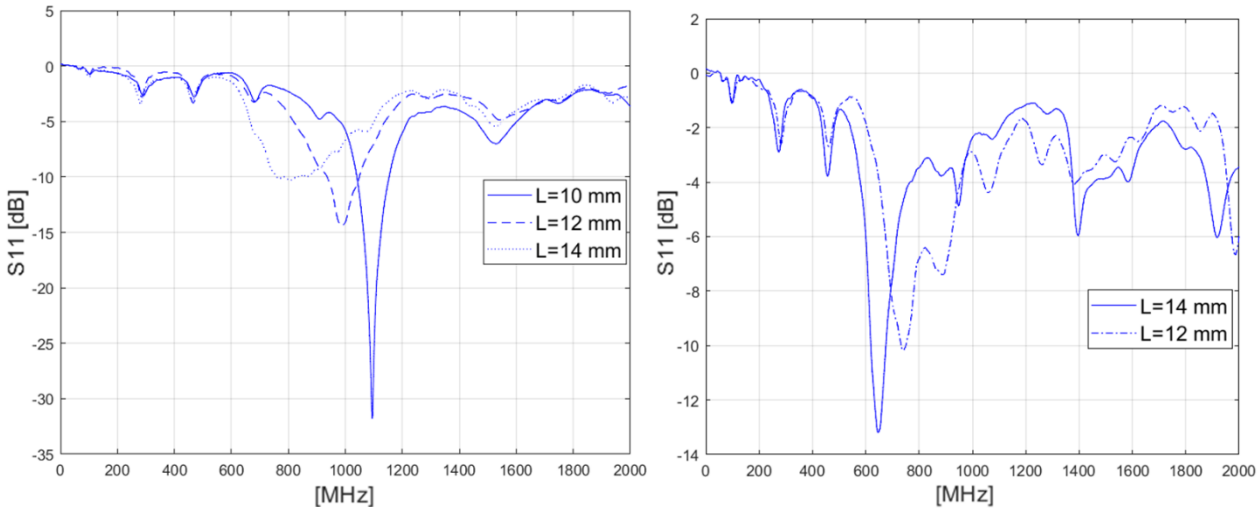

a) *b)*

Fig 3.13: S11 of the machine embroidered bow tie antennas of a) S9, S11, S12 : L=10,12,14 mm (NE, LD, 2D) b) S3, S6 : L=14,12 mm (no edges, LD , 2D)

Fig 3.14a shows the return loss of sample 3 (high density of stitches) and sample 4 (low density of stitches). In both antennas L =14 mm and there are no edges embroidered. The curves are approximately the same as well as the central frequencies.

Generally, having stitching closer together typically boosts antenna efficiency. Yet, this improvement comes with drawbacks: less flexibility and more thread length, which directly leads to higher manufacturing costs. [22]

Given the negligible difference in performance between the high-density and low-density stitch samples, the high-density stitching was found to be unnecessary.

Fig 3.14b compares the return loss of S2 (stitches placed only in one direction) and S6 (stitches placed in 2 directions). In both antennas L=12 mm and there are no edges embroidered. It can be noticed that sample 6 exhibits a central frequency that is approximately 350 MHz higher than that of Sample 6.

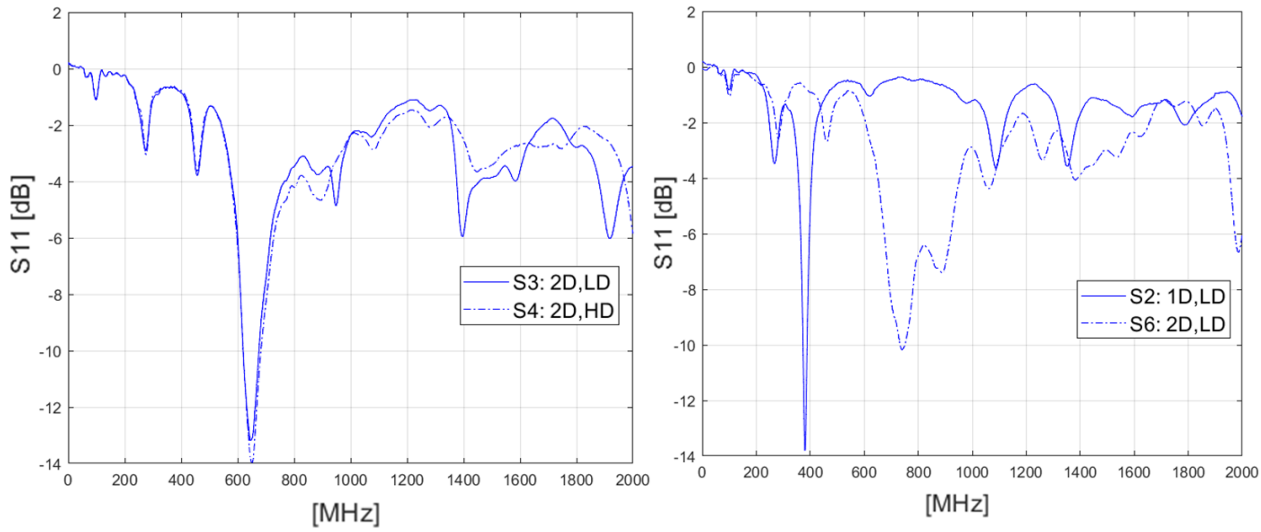

a) *b)*

Fig 3.14: S11 of the machine embroidered bow-tie antennas, comparison of a)Density of stitches S3, S4 b) Direction of stitches S2, S6

When it comes to stitch directions, higher antenna efficiencies can be obtained by ensuring the principal current flow is parallel to the stitch direction. This can lead to further challenges when the design is required to also work at higher modes where the current is in the perpendicular direction and for more complicated designs where the current flows in different directions. [22] Sample 3 is embroidered using two layers of stitching, one on top of the other, with orthogonal directions. Despite having a lower RL it was considered an optimal solution since having two layers ensured more uniform conduction.
This topic will be better addressed in Section 4.2.

From Figure 3.15a and b, it's evident that embroidering the edges of each triangle of the antenna results in a central frequency increase of approximately 200 MHz. However, there's no significant improvement between the sample featuring Zig Zag edges and those with regular edges (Fig 3.15 a and c).

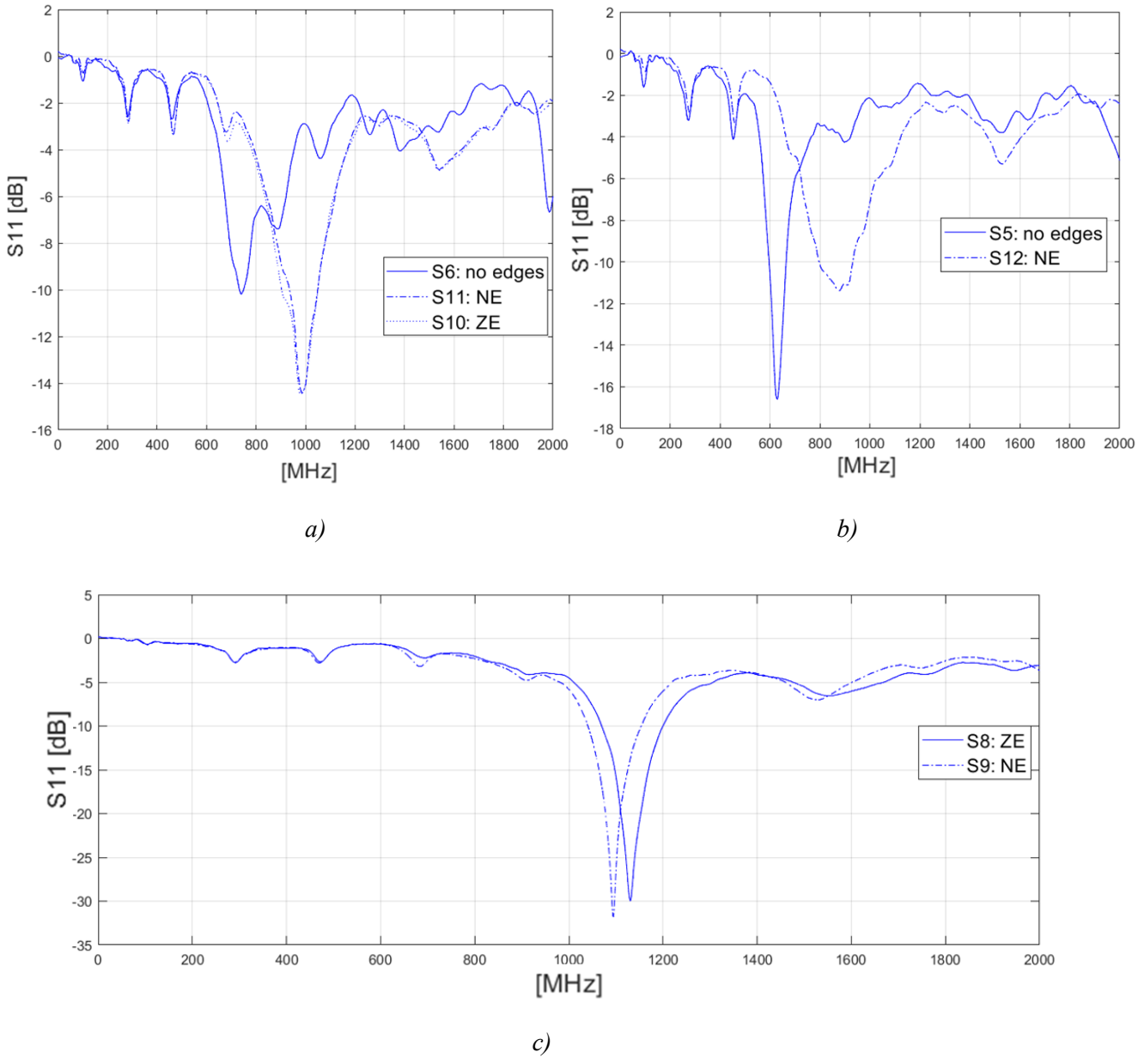

a) *b)*

c)

Fig 3.15: S11 of the machine embroidered bow tie antennas a) (L=12 mm, LD) S6: no edges S11:NE S10: ZE b) (L=14mm ,LD) S5: no edges S12:NE c) (L=10mm,LD) S8:ZE S9=NE

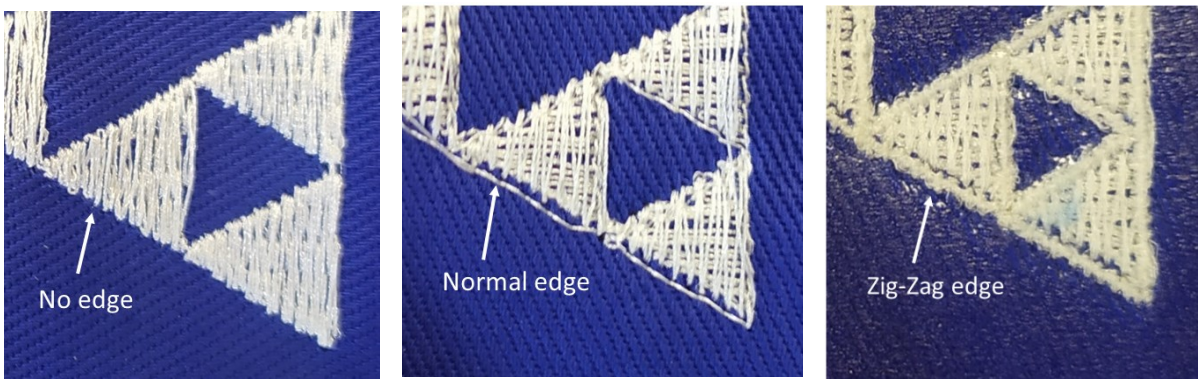

a) b) c)

Fig 3.16: a) no edge b) Normal edge c) Zig-Zag edge

Sample 7 is embroidered using conductive thread on both sides of the substrate fabric. In Fig 3.17 its S11 parameter is compared to the return loss of sample 5 having the same dimensions and features as sample 7 but with a conductive thread only on one side.

The curves are approximately the same as well as the central frequencies.

Introducing conductive thread on both sides doesn't seem to enhance performance significantly, as observed in this analysis. However, this approach does consume more thread, potentially increasing production costs. Moreover, it alters the dielectric properties of the substrate which can influence antenna behavior. Additionally, there's a noticeable reduction in flexibility when using this method, which could be a drawback depending on the application requirements.

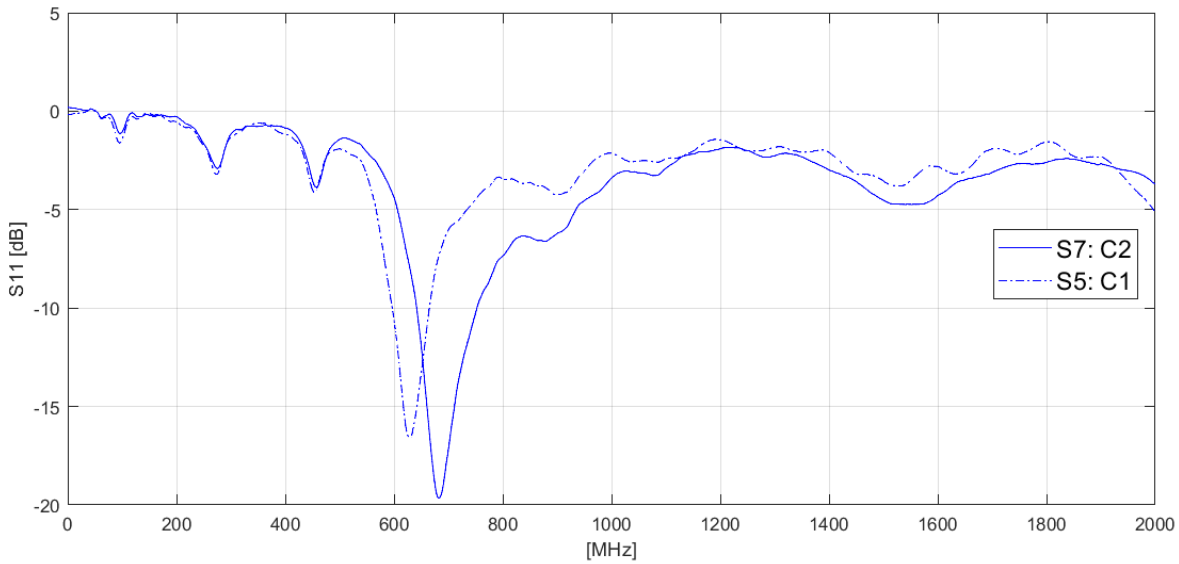

Fig 3.17: S11 of the machine embroidered bow-tie antennas S7: C2 and S5:C1

When it comes to embroidering features such as stitch patterns, densities, and dimensions for antennas, it's important to recognize that they're strongly interrelated. Adding edges, for instance, inevitably modifies the antenna's dimensions, making it slightly bulkier. On the other hand, employing two layers of stitches ensures more uniform conduction, but it will result in tighter stitches, leading to a slightly smaller antenna.

Additionally, it's essential to account for the practical limitations of the embroidery machine. While theoretical adjustments, like a 2 mm increase in dimensions, may seem beneficial, practical limitations might make such changes impercettible.

Finding the right balance between theoretical and practical execution is key in textile electronic. This type of study often involves a trial-and-error process, where theoretical insights meet real-world testing and adjustments.

Sample 12 ultimately met the required specifications making it the final iteration. As previously discussed, Figure 3.18 illustrates that the CST model lacks the multiple peaks characteristic of a fractal antenna, however, it shares the same central frequency as the prototype approximately at 864 MHz. This congruence indicates a solid match between the simulated model and the physical prototype; the CST model is an effective representation of the prototype.

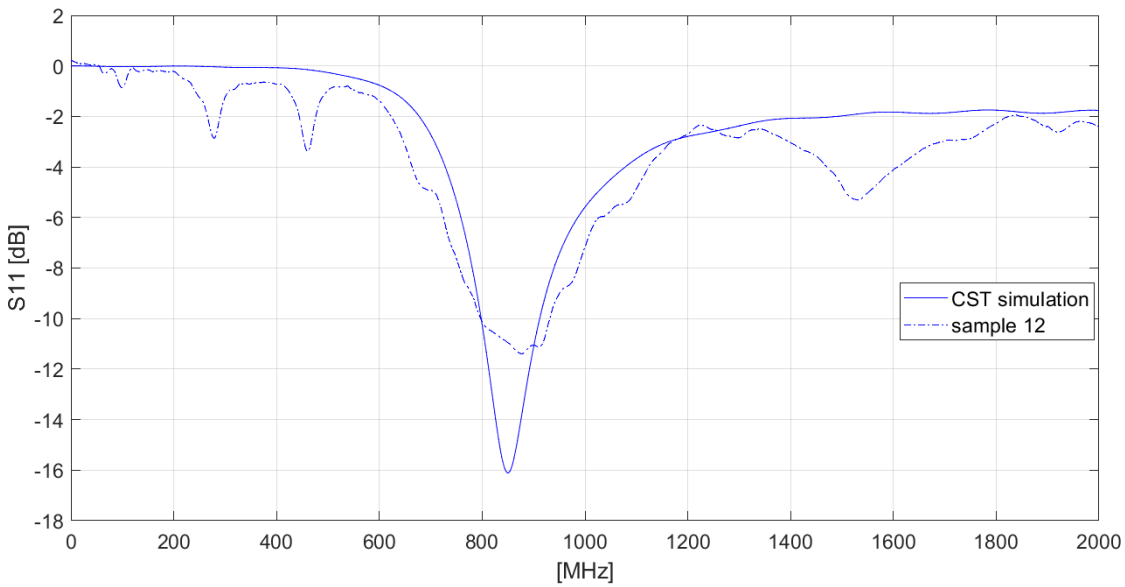

Fig 3.18: S11 of sample 12 (dotted) and the CST model (full)

Based on sample 12, an antenna with identical dimensions and features was also hand embroidered (Sample 13).

To simplify the sewing process, the outer edges of each triangular unit were machine embroidered, leaving the interior to be hand embroidered with conductive thread on one side. This approach naturally led to some disparities between the two samples.

Ideally, ensuring consistent conduction would involve using a single, unbroken piece of conductive thread. However, this isn't possible, so the thread is sewn into sections with nodes to connect them. This inevitably introduces discontinuities and imperfections. Furthermore, the choice of sewing method varied depending on the individual, making it less predictable in terms of performance reliability.

Despite the practical difficulties, the hand-embroidered sample shows a central frequency of 863MHz making it usable for the desired application.

Fig 3.19: Hand embroidered bow tie antenna

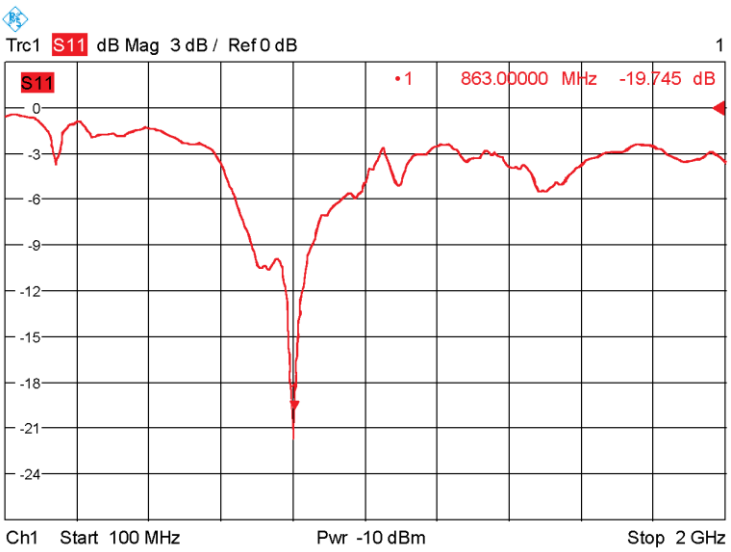

Fig 3.20: S11 of hand-embroidered bow-tie antenna

While the hand-embroidered antenna design could potentially be integrated into the wearable device, it was ultimately dismissed because it was too complex and time-consuming to recreate. Consequently, a smaller and more straightforward alternative is chosen: a dipole antenna, better suited for embroidery.

3.4 FABRICATION PROCESS: DIPOLE ANTENNA

As for the bow tie, the fabrication of the dipole antenna was a trial-and-error process aimed at tuning the frequency to 868 MHz. This iterative approach involved adjusting the following parameters:

- Length of the dipole
- Density of stitches:
  - Hight density (HD)
  - Low density (LD)

Consistency was maintained throughout the process by using the same sewing machine Bernina QE750, Vector Network Analyzer (VNA), and PVC structure for measurements. The antenna was embroidered on the same cotton fabric as the bow tie antenna, and the same coaxial cable and conductive thread were used. Additionally, all measurements were conducted under identical environmental conditions to ensure the accuracy and reliability of the results.

The design of the antenna is illustrated in Fig 3.5 where the values of $d_p = 10\ mm$, $d_w = 5\ mm$, $d_s = 5$ mm were maintained for all samples.

Sample (S)	d_L/2 [mm]	Stitches	Freq [MHz]	RL [dB]
1	70	HD	766	12.7
2	70	LD	805	15.4
3	65	LD	868	12.6
4	65	Hand + HD	780	32
5	57	LD	853-1000	16.5 / 19
6	70	Hand	-	-
7	63	Hand	867	12.6

Tab 3.5: Summary of the characteristics of the dipole antenna prototypes

Fig. 3.21: Hand-embroidered dipole antenna

Fig. 3.22 compares the S11 parameter for samples 5, 3, and 1, with dipole arm lengths of 57 mm, 65 mm, and 70 mm, respectively. Each sample uses a low stitch density. As expected, longer antenna lengths lower resonant frequencies. This occurs because the resonant frequency of an antenna is inversely related to its physical size.

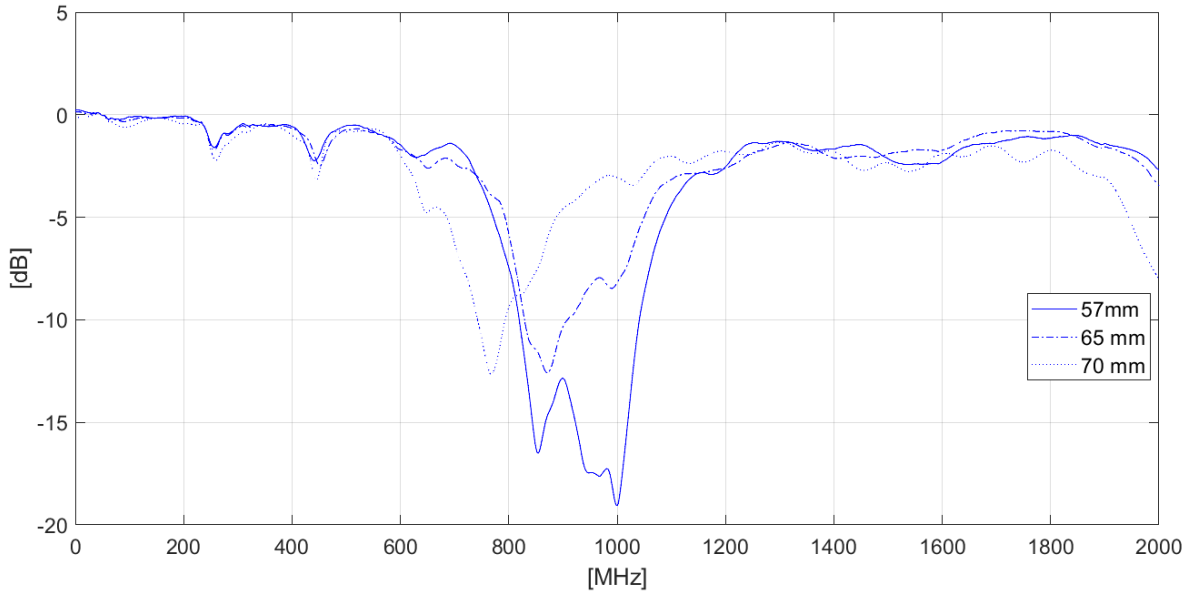

Fig 3.22: Return loss of S_5: dL/2= 57mm; S_3:dL/2=65mm; S_1: dL/2=70mm

Figure 3.23 aims to show how the density of stitches influences the return loss parameter of the antenna. In Figure 3.23a, the S11 parameter is shown for sample 1 and sample 2, with both antennas having the same arm length of 70 mm but embroidered with high and low stitch densities, respectively. Figure 3.23b presents a similar comparison between two dipole antennas with arm lengths of 65 mm, one is hand embroidered with high stitch density and the other one is embroidered by machine with a low stitch density. Both graphs demonstrate that a low stitch density leads to an increase in the central frequency, approximately 50 MHz. While this shift is not large, it consistently shows the same trend in both comparisons.

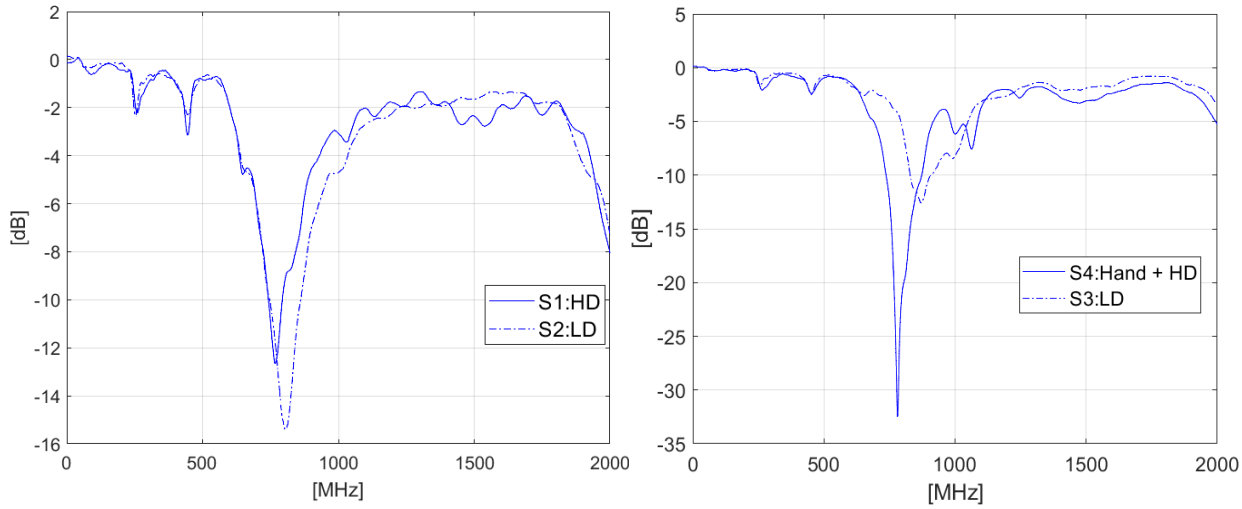

a) *b)*

Fig 3.23: Return loss of a) S1:HD S2: LD b) S4: Hand-embroidered (HD) S3: LD

Figure 3.24 compares the return loss of the CST model, an antenna embroidered by machine, and one embroidered by hand (S6), all with an arm length of 70 mm. The CST model exhibits similar behavior to the machine-embroidered sample, with both showing minima at nearly the same frequency, although their RL differs. In contrast, the hand-embroidered antenna displays multiple peaks, with a RL of 6 dB at the desired frequency of 868 MHz, which makes it unsuitable for the intended application.

The hand-embroidered dipole antenna that met the specified requirement (S7), namely a central frequency of around 868 MHz, has an arm length of 63 mm. Figure 3.25 shows the return loss of two hand-embroidered dipole antennas, each with a length of 63 mm, created by different individuals. It illustrates the consistent reliability of the results, showing that they can be replicated across different embroiderers.

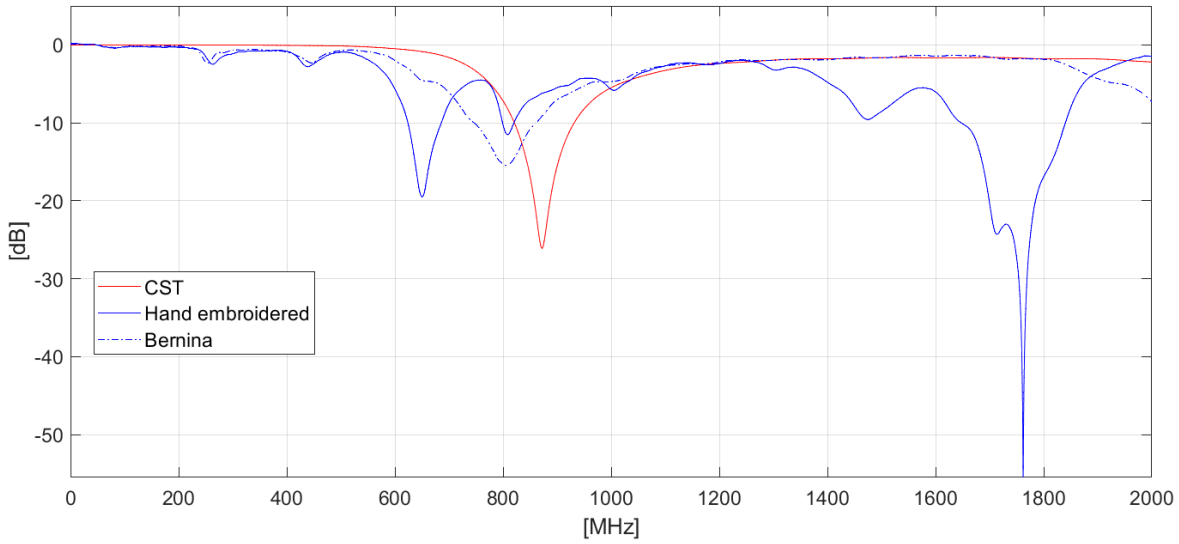

Fig 3.24: Return loss of CST model(red), sample 2 (dotted), hand embroidered dipole antenna (blue)

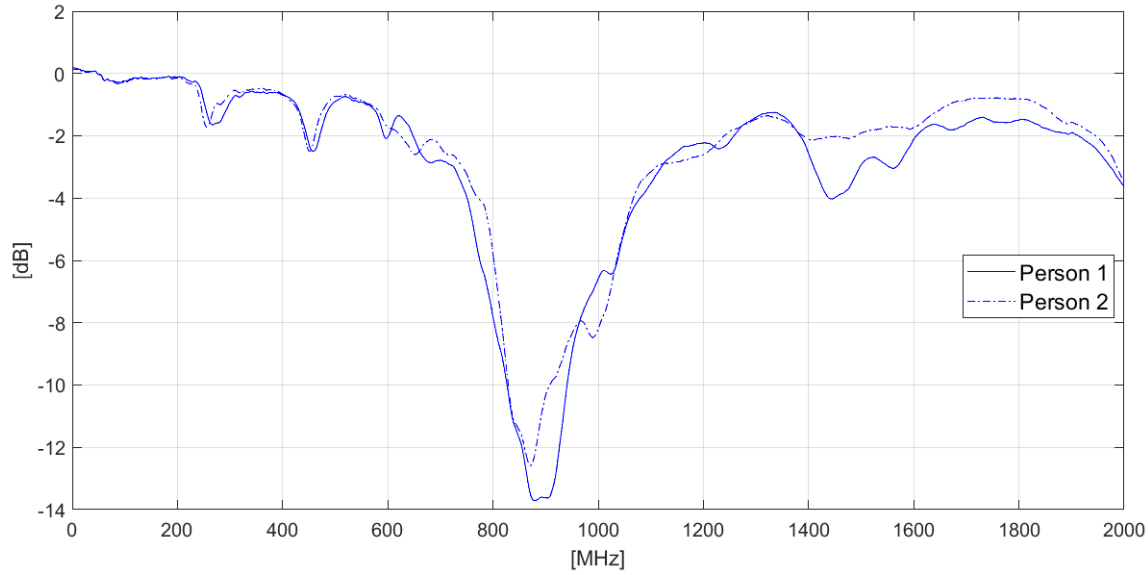

Fig 3.25: S11 of a dipole antenna with an arme length of 63 mm embroidered by two different people.

4

Challenges And Implementation:

Wearable Body-Temperature Monitoring

In this chapter, the technical challenges and solutions related to integrating a coaxial cable with a textile antenna are explored, along with the implementation of the antenna in a body temperature monitoring system. Snap fasteners are investigated as a potential method for connecting the coaxial cable to the textile antenna and a solution to the problem of nonuniform conduction is presented.
Next, the practical application of a body temperature monitoring system that uses the textile antenna is discussed. In this chapter, the LoRaWAN communication protocol is also discussed, detailing its functionality and the reasons for its selection in this project. By the end of this chapter, a comprehensive understanding of the challenges faced, the solutions implemented, and the practical application of the textile antenna in a real-world monitoring system will be provided.

4.1 FEEDING ISSUES

Commercial snaps (clothing fasteners) can be used to connect a coaxial cable to a microstrip line or wearable antenna in this case.
Employing snap fasteners to connect the wearable and electronic components offers the advantage of potential isolation between the two, allowing their disconnection as needed.
They are easy to use, cost-effective and they enable the washing of the wearable component. Additionally, their widespread use in the textile industry means that no additional machinery is required when integrating them into smart clothing designs. They are available in a diverse range

of sizes and designs, from robust options suitable for outdoor apparel to tiny variants as small as 3 mm, snap fasteners offer versatility and adaptability to various applications. [31]
In this study, snap fasteners were incorporated into the feeding method for the dipole antenna. They are commercial off-the-shelf snaps (6.2 mm) of Prym trademark. They are made of aluminum with no coating material.
Two methods to integrate a snap-on feeding arrangement with a coaxial cable in textile antennas are considered:

- The male botton snap fasteners is **crimped** to the textile.
- The male botton snap fasteners is **soldered** to the textile.

In both cases, the female snap is soldered to the coaxial cable.

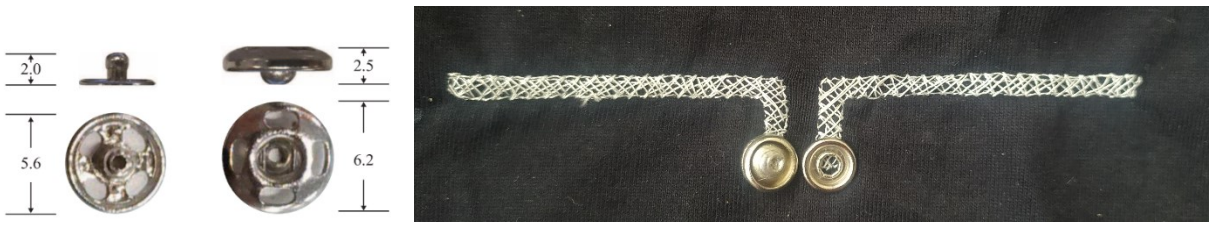

a) *b)*

Fig 4.1: a) Snap fasteners b) Hand embroidered dipole antenna with snap fasteners

Sample	Feeding structure	RL [dB] at 868 MHz
S5	Direct soldering	14.7
S5_1	Crimped snap fasteners	5
S5_2	Soldered snap fasteners	7

Tab 4.1: Return loss at 868 MHz of a dipole antenna with different feeding methods

The return loss of sample 5 of the dipole antenna was evaluated using three different feeding methods: direct soldering of the coaxial cable to the antenna, using crimped snap fasteners (S5_1), and using soldered snap fasteners (S5_2). Figure 4.2 illustrates the comparative results for these three feeding structures.

To achieve high efficiency in an antenna, its impedance must match the characteristic impedance of the coaxial cable. For coaxial-fed patch antennas, this can be done by selecting the appropriate feeding position. However, when snap buttons are used, the impedance of the feeding structure deviates from the characteristic impedance of the coaxial cable. As a consequence, the return loss value in dB is smaller (closer to 0 dB).

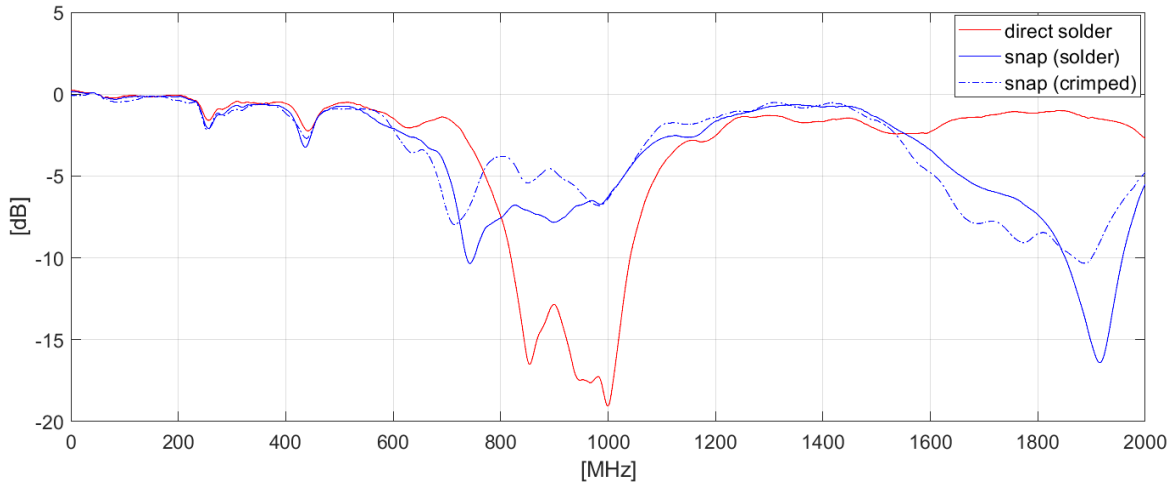

Fig 4.2: Return loss of the dipole antenna with three feeding methods: direct solder (red), soldered snap fasteners (blu) and crimped snap fasteners (dotted)

Despite the advantages, the snaps perform poorly; direct soldering remains the best option.

An issue arises during the soldering process where conductive threads are integrated into the fabric. The heat involved can harm both the thread and the fabric. Although the thread can handle such high temperatures, its delicate nature makes the soldered connection unstable.

Moreover, since the thread is only partially made of metal and sits on top of the fabric, it makes the contact surface uneven and it's likely to detach, especially when bent. This instability weakens the antenna's structure. One way to address this issue is to use UV glue at the feeding points, making them more stable without affecting antenna performance.

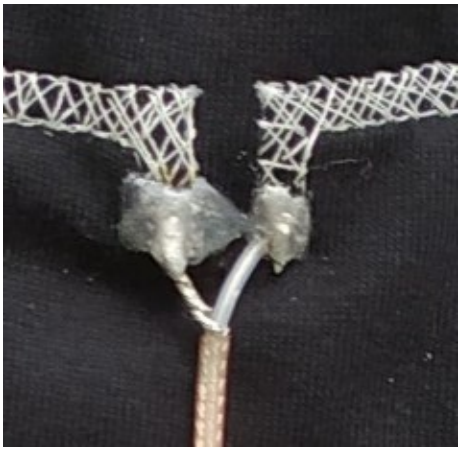

Fig 4.3: Feeding point with coaxial cable directly soldered on the antenna and covered with UV glue

4.2 TPU LAMINATION

When it comes to embroidering or sewing thread onto fabric, it's clear that no matter how tight the stitches are, the thread merely rests on the fabric's surface without fully adhering. Achieving consistent spacing and attachment between threads is also challenging. This presents a potential problem in textile electronics, as it may lead to uneven conduction. Specifically, in the case of a textile antenna, the conductive thread needs to form a uniform conductive surface to ensure proper current flow and radiation of the antenna.

This is particularly important for the bow tie antenna design, where two layers of conductive thread are used without direct contact between them.

One solution to address this issue is to apply a TPU (Thermoplastic Polyurethane) foil over the antenna, in order to compress the threads together and reduce the electrical resistance within the conductive threads. This TPU layer is adhered to the fabric through a heat press method. Importantly, a hole is strategically placed in the middle of the allow the soldering of the feeding line.

In Figure 4.4, two microscope images display the threads of the bow tie antenna before and after lamination. Following lamination, the threads are tightly pressed together, resulting in improved contact and eliminating the space between the two layers of threads observed before lamination.

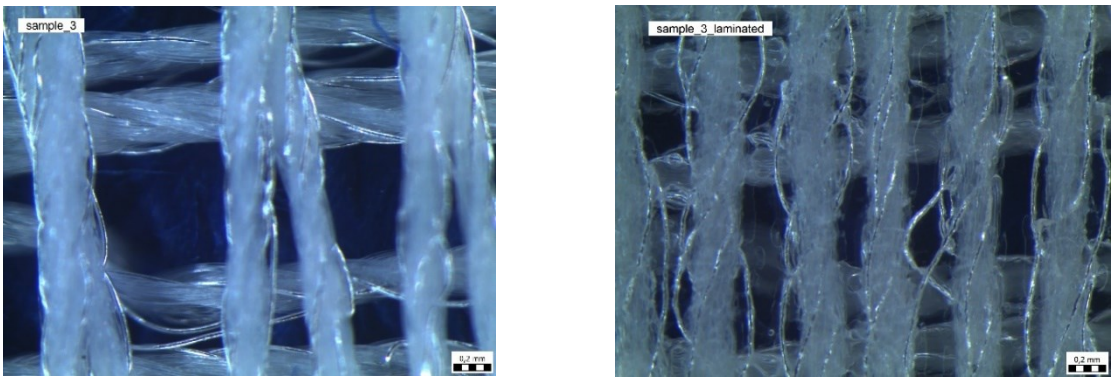

a) b)

Fig 4.4: Conductive thread of bow tie antenna sample 3 a) before TPU lamination b) after TPU lamination

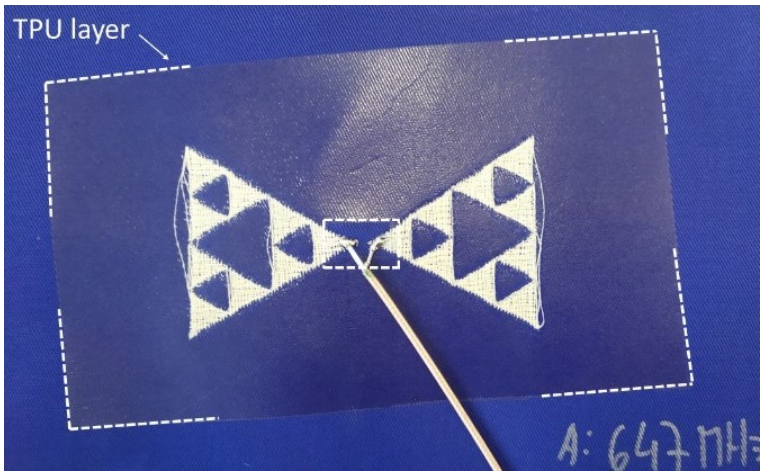

Fig 4.5: Bow-tie antenna with TPU lamination

Introducing an additional layer to the antenna structure inevitably alters its characteristics due to the differences in material properties. For instance, the permittivity of the new material differs from that of the original fabric, thus impacting the antenna's behavior. Moreover, also the size of the lamination affects the system. When the TPU layer is small or thin in size, it has a minimal impact on the overall uniformity of the sample. [32]

It's important to remark that the size of the TPU covering should be tailored to suit the specific needs of the application. In some contexts, priorities may vary, and ensuring freedom of movement might be prioritized to the antenna's washability.

For the bow tie antenna, an investigation into how TPU lamination impacts return loss and resonant frequency has been carried out. The results show that TPU lamination leads to an increase in resonant frequency by approximately 50 MHz, up to a central frequency of 800 MHz and a decrese of the Return loss. However, for frequencies higher than this, the parameters remain roughly the same before and after lamination. When the stitch pattern is thick and dense, ensuring a more even connection, the issue of uneven connection is significantly reduced, making the lamination unnecessary.

Sample	Freq [MHz] before lamination	Freq [MHz] after lamination
3	647	693
4	650	690
6	745	840
7	673-720	862
8	1130	1132.5
12	864	864

Tab 4.2: Bow tie antenna Resonant Frequency comparison before and after TPU lamination.

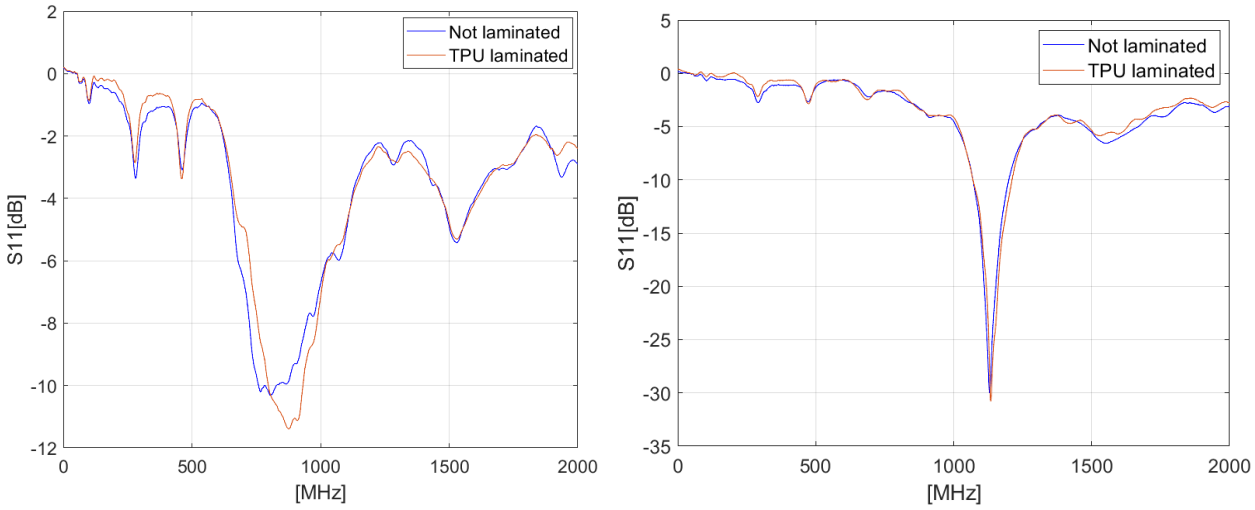

a) *b)*

Fig 4.6: Return loss of bow tie antenna before and after lamination a) Sample 12 b) Sample 8

4.3 SYSTEM INTEGRATION FOR PRACTICAL DEPLOYMENT

The designed textile antenna is integrated into a wearable system to monitor body temperature and transmit the collected data through LoRaWAN connectivity. For this purpose, the CubaCell Htccab02as development board manufactured by Heltec company was selected.

It is a compact, low-power module intended for IoT applications, particularly those requiring long-range wireless communication and energy efficiency.

Designed to be energy-efficient, the board is ideal for battery-powered applications. It is capable of operating for extended periods on a 3.7V lithium battery.

It is also compatible with the Arduino development environment, allowing developers to use the extensive libraries and resources available for Arduino. This drastically simplifies the development process and enables quick prototyping.

To detect body temperature, the waterproof DS18B20 temperature sensor with a probe was used. The probe version was chosen because its long wire is necessary to reach the body, ensuring accurate temperature measurements in our wearable system.

The system was programmed to detect the temperature and send the date every 10 seconds in order to facilitate continuous monitoring and real-time visualization.

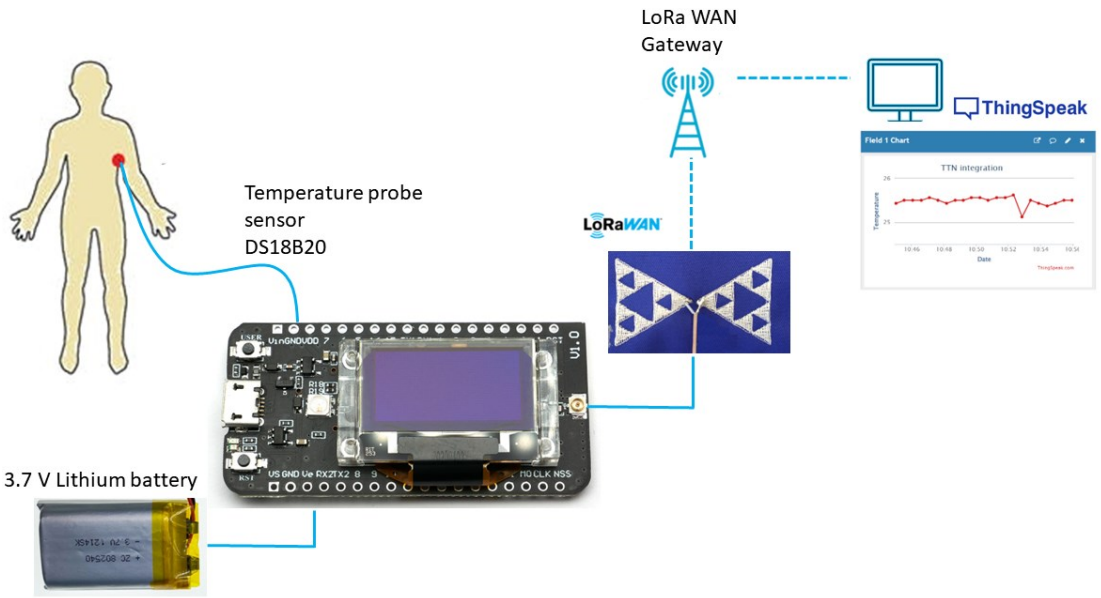

Fig 4.7: Schematic of the wearable system designed to detect body temperature.

To monitor the data transmitted via LoRa, the website *ThingSpeak* was employed. This platform allows the user to view real-time graphs of the transmitted data, providing an immediate and clear visual representation of our information. ThingSpeak is a versatile and user-friendly IoT analytics platform that enables the collection, analysis, and visualization of data from various sources. It supports integration with devices and applications, making it ideal for monitoring and analyzing sensor data, weather data, or any other time-series data. Additionally, ThingSpeak offers MATLAB integration for more advanced data analysis and customized visualizations, enhancing its utility for IoT projects and research.

4.4 LoRaWan COMUNICATION PROTOCOLL

Compared to other electronic systems, embedded systems used in IoT are characterized by:

- Low- power consumption
- Low computing power
- Small size
- Small cost

The most important feature of IoT devices is to transmit data through a wireless network. A variety of protocols are available, allowing the designer to choose based on the required range, bandwidth, and power consumption.

Protocols such as Bluetooth, Wi-Fi, 2G, 3G, 4G, 5G, and NFC are common in the IoT world. These protocols are typically categorized by their bandwidth and range, as shown in Figure 4.8.

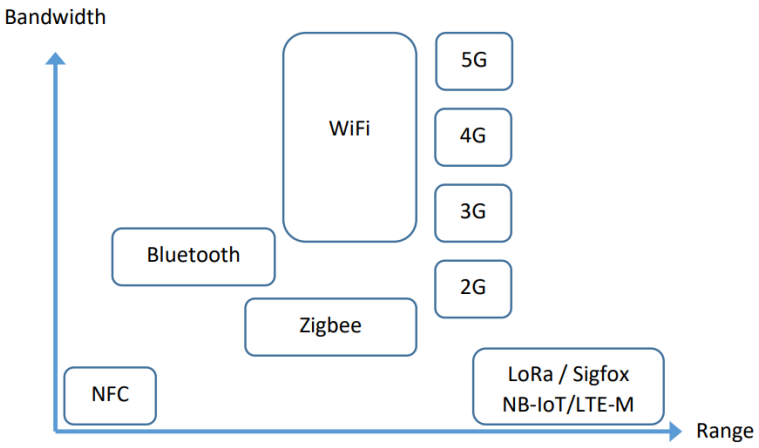

Fig 4.8 Protocols in IoT

Designers generally aim to maximize both range and bandwidth.

LoRa (short for Long Range) is a proprietary modulation technique developed by Semtech Corporation. It enables long-range communication with low power consumption, making it suitable for Internet of Things (IoT) applications. In other words, LoRa serves as the modulation method used in communication between two LoRa-enabled devices or between a device and a gateway. However, when considering the entire communication process, spanning from the device to the LoRaWAN server, it refers to the LoRaWAN (Long Range Wide Area Network)

standard. LoRaWAN expands upon the LoRa protocol by enabling secure connectivity between devices and servers, facilitating data delivery to end-users.

- LoRa physical layer: Type of modulation (Chirp Spread Spectrum) and the physical frame
- LoRaWAN standard: Network architecture (end-device, gateways, servers) and a more specific frame format allowing a LoRaWAN end-device to securely transmit data to a LoRaWAN server.

LoRaWAN is known for its long range and low power consumption, belonging to the group known as Low Power Wide Area Networks (LPWANs).
In Europe, certain frequency bands are available for public use. This implies that no authorization is required and they are free of charge. LoRa can operate on the 433 MHz, 868 MHz, or 2.4 GHz bands in Europe, but only the 868 MHz band is utilized for LoRaWAN.
Fig 4.9 shows the entire LoRaWAN architecture.

Band	Protocols
13.56 MHz	RFID, NFC
433 MHz	Walkie-talkie, remote control, LoRa
868 MHz	Sigfox, LoRa
2.4 GHz	Wi-Fi,Bluetooth, Zigbee,LoRa
5 GHz	Wi-Fi

Tab 4.3: Free frequency bands

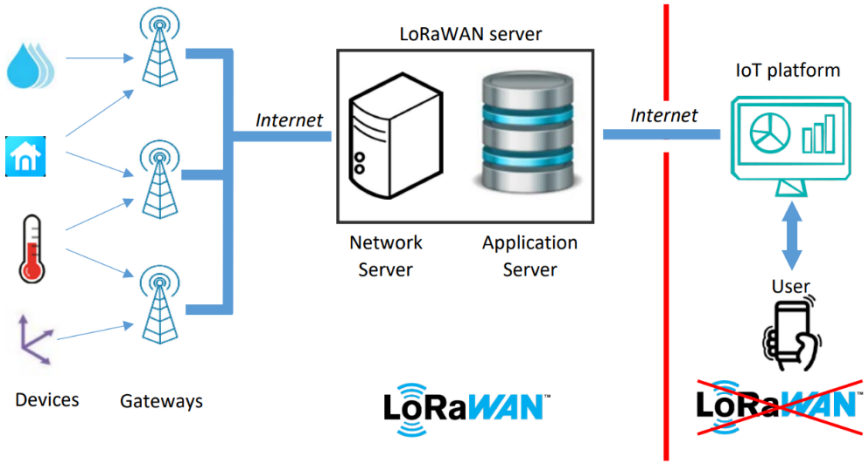

Fig 4.9: LoRaWAN architecture

LoRaWAN end devices are equipped with a LoRa radio transceiver, they communicate with each other or with gateways. Unlike traditional setups where devices communicate exclusively with a single gateway, LoRaWAN end devices transmit messages that are received and processed by all gateways within the coverage area.

Typically LoRa provides for long-range communications up to five kilometers in urban areas, and up to 15 kilometers or more (line of sight). [33]

The LoRaWAN gateway simultaneously monitors all channels and forwards its contents over the Internet to the Network Server, configured beforehand. It captures LoRa-modulated signals via its antenna and then connects to the Internet using various available backhaul options such as Wi-Fi, 3G, 4G, 5G, and Ethernet.

Gateways are typically deployed by various entities such as businesses, government agencies, or community organizations but finding a free one in a big city is not always guaranteed. If there are no free gateways available, setting a personal gateway will be necessary to establish connectivity for your IoT devices. Each gateway has a unique identifier (64 bits EUI). This ID is useful to register and activate a gateway on a Network Server.

Afterward, the messages transmitted by the gateways are received by the Network Server, which eliminates duplicate packets (because multiple gateways may receive and transmit the same message to the Network Server). Then, the Network Server authenticates the message using a

128-bit AES key, known as *NwkSKey* (Network Session Key). If the authentication process succeeds, the Network Server transfers the encrypted message to the Application Server.
The IoT platform is the user application interface, it connects with the Application Server to collect the data. Most of the time, this is done either thanks to the HTTP or the MQTT protocol.
An IoT platform is not specific to the LoRaWAN standard, its role is to store the data in a database, present them in different forms (tables, graphs…), and finally make them available through a web service that the user can query. The transfer of data can occur in both directions: the IoT platform can receive data from the LoRaWAN server (uplink) (mostly used) or it can transmit the data to the LoRaWAN server (downlink). [34]
One widely used IoT platform is *ThingSpeak*. Developed by MathWorks, it integrates seamlessly with MATLAB, allowing users to perform advanced data analysis and visualization directly within the ThingSpeak environment.

4.5 FINAL RESULTS

This section presents the final results of the research, detailing the development and evaluation of two prototype textile antennas. These prototypes are the result of various analyses and trials conducted throughout this thesis. Both antennas were designed to operate at 868 MHz, which is a key frequency for the chosen application. The successful implementation of these antennas demonstrates the viability of textile-based solutions for wearable system.
This research focused on creating antennas that are both functional and seamlessly integrated into wearable textiles. The following sections describe the two prototype antennas that were developed: an embroidered bow-tie antenna and an embroidered dipole antenna.
The embroidered bow tie antenna was designed with a symmetrical bow tie shape, incorporating a fractal Sierpinski geometry. This design choice is known for its broad bandwidth and efficient radiation properties. The side of the smaller triangle in the fractal design measures 14 mm. The embroidery process involved using conductive threads to form the antenna pattern on a textile substrate. Both hand-embroidered and machine-embroidered versions were produced, and both achieved similar results.

For the machine-embroidered version, stitches were applied in two directions with low density, and the edges were sewn with a normal stitch. For feeding, a coaxial cable was directly soldered to the antenna, and glue is added at the feeding point to ensure stability.
The embroidered dipole antenna, a more traditional antenna design, was also developed. The dipole configuration consists of two conductive elements arranged in a straight line with a feed point in the center. Similar to the bow tie antenna, conductive threads were used to create the dipole pattern on a textile base, ensuring the antenna was tuned to the desired frequency of 868 MHz.
For this antenna, the feeding setup was the same as the bow tie antenna, using a coaxial cable directly soldered to the antenna with glue added at the feeding point for stability. The embroidery stitches were applied in two directions with low density, similar to the bow tie antenna.

Return loss measurements indicated that both antennas exhibited acceptable impedance matching at the target frequency of 868 MHz, making them suitable for the desired application.
Based on the prototypes developed, a workshop entitled "*Smart Stitchers*" was conducted in Regensburg. The workshop aimed to introduce students, particularly girls, to the STEM fields, with a focus on electronics. Fourteen girls, all under the age of 14, participated in the workshop, implementing their own wearable systems.
Due to the time-consuming nature of the hand-embroidering bow-tie antenna, the dipole solution was chosen for the workshop. Each student successfully embroidered their own dipole antenna and assembled the device, which included the temperature sensor. They soldered the feeding network, connected all components together, and completed the assembly. By the end of the workshop, every system was working successfully.
The "Smart Stitchers" workshop demonstrated how textile electronics and wearable systems are accessible even to non-experts. It showcased that, following an initial design and analysis process, such systems can be easily put together. This hands-on experience empowered the students and provided them with practical insights into electronics and wearable technology.

Fig 4.10: Workshop flyer

5

Conclusions and Future Works

5.1 CONCLUSIONS

This thesis has demonstrated the potential of textile antennas through the design, fabrication, and testing of two specific antenna types: a bow tie with Sierpinski geometry and a half-wave dipole antenna. The focus was not merely on theoretical exploration but on practical implementation, showing the capabilities and challenges associated with textile antennas.

Through a series of prototypes, the embroidering fabrication techniques was explored, including different stitching patterns, edge stitching techniques, and feeding methods. The results from these laboratory experiments provided valuable insights into how to optimize the antenna performance and its reliability in wearable applications.

The analysis of both antenna designs revealed several key findings. Using a high density of stitches instead of a low one did not result in significant changes, although there was a slight decrease in the resonant frequency, a fact not particularly relevant. However, the direction of the stitches brought noticeable changes. As suggested in the literature, antenna efficiencies can be improved by ensuring that the principal current flow is parallel to the stitch direction. Adding stitches to the edges was crucial for providing a more uniform connection within the antenna, though a standard stitch at the edge proved sufficient.

Additionally, the results showed great performance when comparing the hand-embroidered equivalent for both designs. This comparison underlines the effectiveness and practicality of using machine embroidery to produce textile antennas, achieving results comparable to those of hand-embroidered counterparts.

A key part of this research was the successful implementation of the textile antenna in a wearable system equipped with a temperature sensor. This system effectively transmitted data using LoRa connectivity, showing the practical utility of these antennas in health monitoring and other wearable technology applications.

An important outcome of this research was the hands-on workshop conducted, where students were able to create their own textile antennas. This aspect of the project highlighted that, with proper guidance and tools, textile antennas can be easily fabricated by non-expert users.

The ability to produce functional textile antennas through relatively simple and accessible methods signifies a substantial advancement in wearable technology. It opens up possibilities for widespread adoption in various fields, from healthcare to consumer electronics, by making the technology accessible to a broader audience.

5.2 FUTURE WORKS

Regarding the antennas designed and tested in this project, several paths for future research and development can be pursued to a deeper understanding of the performance of textile antennas.

A logical continuation of this research is to study the behavior of the antennas when in close proximity to the human body. This could involve creating a detailed model using simulation software that includes the human body to predict how body interaction affects antenna performance. Such simulations would provide valuable insights into optimizing antenna designs for real-world wearable applications.

Another potential direction is to recreate the same antenna designs using different fabrication techniques, such as printing or knitting. Comparing the results with those obtained through the embroidering technique would highlight the strengths and limitations of each method.

Since the dielectric properties were not measured in this project, future work should focus on characterizing these properties accurately. This will help in selecting the best materials and improving the consistency and performance of the antennas.

Finding a reliable solution for a detachable feeding technique is essential to ensure the washability of the wearable system. The use of snap fasteners was explored but proved ineffective. Future research should aim to develop or identify a robust and user-friendly detachable feeding mechanism that maintains good electrical contact while allowing for easy removal during washing.

Despite being available for nearly two decades, the adoption of wearable technologies into everyday use has been slower than anticipated, primarily due to a combination of technological limitations and insufficient market demand.

The increasing demand for wireless connectivity necessitates antennas in nearly every device. Currently, electronics and batteries are rigid components, accommodating the inclusion of rigid antennas without significant inconvenience, especially with small PIFAs operating at 2.4 GHz. Many experts anticipate the next evolutionary trend to be the widespread adoption of truly wearable technology seamlessly integrated into clothing, where textile antennas will play a crucial role.

As electronic components continue to decrease in size, emerging technologies may enable textiles to harness energy themselves.

By employing textiles for antennas, the constraints on size shift from the device dimensions to the wearer's torso. This flexibility in size constraints can potentially improve antenna performance, particularly for lower frequencies with longer wavelengths.

Appendix: Arduino code for Temperature Measurement System

```
#include "LoRaWan_APP.h"
#include <DallasTemperature.h>
#include <Wire.h>
#include "HT_SSD1306Wire.h"

SSD1306Wire  Display(0x3c, 500000, SDA_OLED, SCL_OLED, GEOMETRY_128_64, RST_OLED); //
addr , freq , SDA, SCL, resolution , rst

// Data wire is plugged into GPIO2 on the ESPR32 Board
#define ONE_WIRE_BUS 2

// Setup a oneWire instance to communicate with any OneWire devices (not just
Maxim/Dallas temperature ICs)
OneWire oneWire(ONE_WIRE_BUS);

// Pass our oneWire reference to Dallas Temperature.
DallasTemperature sensors(&oneWire);

/* OTAA para*/
uint8_t devEui[] = { 0x70, 0xB3, 0xD5, 0x7E, 0xD0, 0x06, 0x20, 0x37 };
uint8_t appEui[] = { 0x00, 0x00, 0x00, 0x00, 0x00, 0x00, 0x00, 0x00 };
uint8_t appKey[] = {0xA4, 0x2A, 0x26, 0xDE, 0xFB, 0x33, 0xBD, 0x26, 0xA4, 0xA8, 0x45,
0x93, 0xC8, 0x53, 0x8D, 0x40 };

/* ABP para*/
uint8_t nwkSKey[] = { 0x15, 0xb1, 0xd0, 0xef, 0xa4, 0x63, 0xdf, 0xbe, 0x3d, 0x11,
0x18, 0x1e, 0x1e, 0xc7, 0xda,0x85 };
uint8_t appSKey[] = { 0xd7, 0x2c, 0x78, 0x75, 0x8c, 0xdc, 0xca, 0xbf, 0x55, 0xee,
0x4a, 0x77, 0x8d, 0x16, 0xef,0x67 };
uint32_t devAddr =  ( uint32_t )0x007e6ae1;

/*LoraWan channelsmask, default channels 0-7*/
uint16_t userChannelsMask[6]={ 0x00FF,0x0000,0x0000,0x0000,0x0000,0x0000 };

/*LoraWan region, select in arduino IDE tools*/
LoRaMacRegion_t loraWanRegion = ACTIVE_REGION;

/*LoraWan Class, Class A and Class C are supported*/
DeviceClass_t  loraWanClass = CLASS_A;

/*the application data transmission duty cycle.  value in [ms].*/
uint32_t appTxDutyCycle = 10000;
```

```
/*OTAA or ABP*/
bool overTheAirActivation = true;
/*ADR enable*/
bool loraWanAdr = true;
/* Indicates if the node is sending confirmed or unconfirmed messages */
bool isTxConfirmed = true;
/* Application port */
uint8_t appPort = 2;
uint8_t confirmedNbTrials = 4;
/* Prepares the payload of the frame */
static void prepareTxFrame( uint8_t port )
{
  pinMode(Vext, OUTPUT);
  digitalWrite(Vext, LOW);

  sensors.requestTemperatures(); // Send the command to get temperatures
  float temperature = (float) (sensors.getTempCByIndex(0));
  int int_temp=temperature*100;

  digitalWrite(Vext, HIGH);

  appDataSize = 2;
  appData[0] = int_temp >> 8;
  appData[1] = int_temp;

  Serial.print("Temperature is: ");
  Serial.println(temperature);
  Display.clear();
  Display.drawString(0,0,"Temperature: "+ String(temperature)+" °C");
  Display.display();

}

void setup() {
  Serial.begin(115200);
  Display.init();

  Display.setFont(ArialMT_Plain_10);
  sensors.begin();
  Mcu.begin();
   deviceState = DEVICE_STATE_INIT;
}
void loop()
{
  switch( deviceState )
  {
    case DEVICE_STATE_INIT:
    {
```

```
#if(LORAWAN_DEVEUI_AUTO)
      LoRaWAN.generateDeveuiByChipID();

#endif

      LoRaWAN.init(loraWanClass,loraWanRegion);
      break;
    }
    case DEVICE_STATE_JOIN:
    {
      LoRaWAN.join();
      break;
    }
    case DEVICE_STATE_SEND:
    {
      prepareTxFrame( appPort );
      LoRaWAN.send();
      deviceState = DEVICE_STATE_CYCLE;
      break;
    }
    case DEVICE_STATE_CYCLE:
    {
      // Schedule next packet transmission
      txDutyCycleTime = appTxDutyCycle + randr( -APP_TX_DUTYCYCLE_RND,
       APP_TX_DUTYCYCLE_RND );
      LoRaWAN.cycle(txDutyCycleTime);
      deviceState = DEVICE_STATE_SLEEP;
      break;
    }
    case DEVICE_STATE_SLEEP:
    {
      LoRaWAN.sleep(loraWanClass);
      break;
    }
    default:
    {
      deviceState = DEVICE_STATE_INIT;
      break;
    }
  }
}
```

References

[1] Balanis, Constantine A. "*Antenna Theory: Analysis and Design"* 3rd ed. Hoboken, NJ: John Wiley, 2005.

[2] IEEE "*Standard Definitions of Terms for Antennas"* pp. 145-1983 (Revision of ANSI/IEEE Std 145-1973)

[3] D. A. Abd El-Aziz, T. G. Abouelnaga, E. A. Abdallah, M. El-Said, Yaser S. E. Abdo (2016) "*Analysis and Design of UHF Bow-Tie RFID Tag Antenna Input Impedance"* Open Journal of Antennas and Propagation,04,85-107.

[4] Stutzman, W. L. and Thiele, G. A. „ *Antenna Theory and Design* " John Wiley Sons, 1998.

[5] Coevorden, C.Md.J. van, Amelia Rubio Bretones, Mario Fernández Pantoja, Francisco Javier García Ruiz, Salvador González García and Rafael Gómez Martín. *"GA design of a thin-wire bow-tie antenna for GPR applications*" In *IEEE Transactions on Geoscience and Remote Sensing* 44 (2006) pp.1004-1010.

[6] Olabisi O., Adewumi A. S, Ajao O. S, Adeniran A. O *"Bow-Tie Microstrip Patch Antenna – Design and Implementation for Dual Band WLAN Applications"* in *International Journal of Trend in Scientific Research and Development* (ijtsrd), Volume-3, Issue-4, June 2019, pp.1136-1140.

[7] Ge, Jinjin and Long Jin. *"A Compact Multiband Bow-Tie Dipole Slot Antenna for WLAN and WiMAX Applications"* in *Progress in Electromagnetics Research Letters* 56 (2015): 17-23.

[8] H. M. P. B. Ranasinghe, S. M. P. Senanayake, U. I. P. Senarathne, A. U. A. W. Gunawardena and D. N. Uduwawala, "*Design of a low cost cavity backed wideband bow-tie antenna for ground penetrating radar systems,"* in *IEEE 8th International Conference on Industrial and Information Systems,* Peradeniya, Sri Lanka, 2013, pp. 370-375.

[9] Yang, Xinhuan, John Chiochetti, Dimitris Papadopoulos and Leon Susman. "*Fractal Antenna Elements and Arrays"* in *Applied Microwave & Wireless* May 1999, pp.34-46 .

[10] J. Romeu and J. Soler, *"Generalized Sierpinski fractal multiband antenna*," in *IEEE Transactions on Antennas and Propagation*, vol. 49, no. 8, pp. 1237-1239, Aug. 2001.

[11] P. S. Kirubavathy and K. Ramprakash, *"Design of Sierpinski Fractal Antenna for wideband applications,"* in *International Conference on Innovations in Information, Embedded and Communication Systems (ICIIECS)*, Coimbatore, India, 2017, pp. 1-4.

[12] Bikash Ranjan Behera, "*Sierpinski Bow-Tie antenna with genetic algorithm"* Engineering Science and Technology, an International Journal, Volume 20, Issue 2,2017, Pages 775-782.

[13] C. Puente-Baliarda, J. Romeu, R. Pous and A. Cardama, *"On the behavior of the Sierpinski multiband fractal antenna"* in *IEEE Transactions on Antennas and Propagation*, vol. 46, no. 4, pp. 517-524, April 1998.

[14] Brown, George H. and Woodward, O. M.."*Experimentally Determined Radiation Characteristics of Conical and Triangular Antennas*." RCA Review 13 , no. 4 (1952), pp.425--452.

[15] E. O. Thorp, *"The invention of the first wearable computer" Digest of Papers. Second International Symposium on Wearable Computers (Cat. No.98EX215)*, Pittsburgh, PA, USA, 1998, pp. 4-8.

[16] J. Cannan and H. Hu, *"A wearable sensor fusion armband for simple motion control and selection for disabled and non-disabled users"* in *2012 4th Computer Science and Electronic Engineering Conference (CEEC)*, Colchester, UK, 2012, pp. 216-219.

[17] Jesus Favela 2017 *"Inferring Human Behavior using Mobile and Wearable Devices"* in Proceeding of the 23rd Brazillian Symposium on Multimedia and the Web (WebMedia'17). Association for the Computing Machinery, New York, NY, USA, pp11-13.

[18] Svertoka, E.; Saafi, S.; Rusu, A.; Burget, R.; Marghescu, I.; Hosek, J.; Ometov, A. *"Wearables for Industrial Work Safety: A Survey"* in *Sensors* 2021, 21, 3844.

[19] A. P. Ghodake and B. G. Hogade, *"Textile Antenna –Structure, Material and Applications," 2022* in *International Conference on Electronics and Renewable Systems (ICEARS)*, Tuticorin, India, 2022, pp. 1855-1860.

[20] Jalil, Mohd Ezwan B, Mohamad Kamal Abdul Rahim, Noor Asmawati Samsuri, Noor Asniza Murad, Huda Bin A Majid, Kamilia Kamardin and Muhamad Azfar Abdullah. *"Fractal KOCH multiband textile antenna performance with bending, wet conditions and on the human body"* in *Progress in Electromagnetics Research-pier* 140 (2013) pp. 633-652.

[21] Mehmann, A., Varga, M., & Tröster, G. (2017) "Reversible contacting for smart textiles" In S. Schneegass & O. Amft (Eds.) *Smart textiles: Fundamentals design and interaction*. Cham: Springer.

[22] Tsolis, A.; Whittow, W.G.; Alexandridis, A.A.; Vardaxoglou, J.C. *"Embroidery and Related Manufacturing Techniques for Wearable Antennas: Challenges and Opportunities"* in *Electronics* 2014, vol. 3, pp. 314-338.

[23] I. Locher, M. Klemm, T. Kirstein and G. Troster, *"Design and Characterization of Purely Textile Patch Antennas"* in *IEEE Transactions on Advanced Packaging*, Nov. 2006. vol. 29, no. 4, pp. 777-788,.

[24] P. Banerjee, G. Ghosh and S. K. Biswas, *"A simple technique for the measurement of the permittivity of medium loss samples using cavity perturbation method,"* in *IEEE Applied Electromagnetics Conference (AEMC)*, Kolkata, India, 2007, pp. 1-3.

[25] Rohde & Schwarz *"Measurement of Dielectric Material Properties"* Application Note, version 5, 23 May 2012.

[26] K. W. Kark. *"Antennen und Strahlungsfelder: Elektromagnetische Wellen auf Leitungen im Freiraum und ihre Abstrahlung"* 8th ed. Wiesbaden: Springer Vieweg, 2020.

[27] Marterer, V., Radouchová, M., Soukup, R. *"Wearable textile antenna: investigation on material variants, fabrication methods, design and application"* in *Fash Text* 11,9 (2024).

[28] Priya, Ankita, Ayush Kumar, and Brajlata Chauhan. *"A Review of Textile and Cloth Fabric Wearable Antennas"* in *International Journal of Computer Applications* 116, no. 17 (2015) pp.1-5.

[29] Kellomäki, T, "*Effects of the Human Body on Single-Layer Wearable Antennas*" Tampere University of Technology. Publication, 2012, vol. 1025.

[30] Stoltz, H., Ribi, S., *"Bernina 750 QE Manual"* 2012 BERNINA International AG, CH-Steckborn.

[31] Kellomäki, T. (2012) "*Snaps to Connect Coaxial and Microstrip Lines in Wearable Systems"* in *International Journal of Antennas and Propagation*, *2012*, 1-10. Article 659287.

[32] Veske, P.; Bossuyt, F.; Vanfleteren, J. *"Testing for Wearability and Reliability of TPU Lamination Method in E-Textiles"* in *Sensors* 2022, vol. 22, pp.156.

[33] Semtech "*LoRa and LoRaWAN: A Technical Overview*", Technical paper, December 2019.

[34] Sylvain Montagny, "*LoRa - LoRaWAN and Internet of Things for beginners"* Savoie Mont Blanc University.